THE JOURNAL OF BIOLOGICAL CHEMISTRY VOL. 289, NO. 43, pp. 29892–29911, October 24, 2014

Gene Targeting Study Reveals Unexpected Expression of Brain-expressed X-linked 2 in Endocrine and Tissue Stem/Progenitor Cells in Mice*

Received for publication, May 13, 2014, and in revised form, August 13, 2014 Published, JBC Papers in Press, August 20, 2014, DOI 10.1074/jbc.M114.580084

Keiichi Ito[‡], Satoshi Yamazaki[‡], Ryo Yamamoto[‡§], Yoko Tajima[‡], Ayaka Yanagida[‡], Toshihiro Kobayashi[¶‖], Megumi Kato-Itoh[‡¶], Shigeru Kakuta[**], Yoichiro Iwakura[‡‡], Hiromitsu Nakauchi[‡§¶], and Akihide Kamiya[‡§§1]

From the [‡]Division of Stem Cell Therapy, Center for Stem Cell and Regenerative Medicine, Institute of Medical Science, University of Tokyo, Minato-ku, Tokyo 108-8639, Japan, the [¶]NAKAUCHI Stem Cell and Organ Regeneration Project, Japan Science and Technology Agency, Chiyoda-ku, Tokyo 102-8666, Japan, the [‖]Wellcome Trust Cancer Research UK Gurdon Institute, University of Cambridge, Cambridge CB2 1QN, United Kingdom, the [**]Department of Biomedical Science, Graduate School of Agriculture and Life Sciences, University of Tokyo, Bunkyo-ku, Tokyo 113-8657, Japan, the [‡‡]Center for Animal Disease Models, Research Institute for Biomedical Sciences, Tokyo University of Science, 2669 Yamazaki, Noda, Chiba 278-0022, Japan, the [§]Institute for Stem Cell Biology and Regenerative Medicine, Stanford University School of Medicine, Stanford, California 94305, and the [§§]Laboratory of Stem Cell Therapy, Institute of Innovative Science and Technology, Tokai University, 143 Shimokasuya, Isehara, Kanagawa 259-1143, Japan

Background: The role and precise expression pattern of individual brain-expressed X-linked genes *in vivo* were unknown.
Results: Bex2-EGFP knock-in–knock-out mice were viable and fertile. Outside the brain, EGFP was expressed in specific cell populations.
Conclusion: Bex2 plays redundant roles *in vivo* but is specifically expressed in endocrine and stem/progenitor cells.
Significance: Bex2 is a novel marker for endocrine and stem/progenitor cells.

Identification of genes specifically expressed in stem/progenitor cells is an important issue in developmental and stem cell biology. Genome-wide gene expression analyses in liver cells performed in this study have revealed a strong expression of X-linked genes that include members of the brain-expressed X-linked (*Bex*) gene family in stem/progenitor cells. Bex family genes are expressed abundantly in the neural cells and have been suggested to play important roles in the development of nervous tissues. However, the physiological role of its individual members and the precise expression pattern outside the nervous system remain largely unknown. Here, we focused on Bex2 and examined its role and expression pattern by generating knock-in mice; the enhanced green fluorescence protein (*EGFP*) was inserted into the *Bex2* locus. *Bex2*-deficient mice were viable and fertile under laboratory growth conditions showing no obvious phenotypic abnormalities. Through an immunohistochemical analysis and flow cytometry-based approach, we observed unique EGFP reporter expression patterns in endocrine and stem/progenitor cells of the liver, pyloric stomach, and hematopoietic system. Although Bex2 seems to play redundant roles *in vivo*, these results suggest the significance and potential applications of Bex2 in studies of endocrine and stem/progenitor cells.

Studies on chromosomal assignment of the genes expressed during hematopoiesis have shown that stem cell-specific genes are located on the X chromosome more frequently than are differentiated cell-specific genes (1). The X chromosome is similar to autosomal chromosomes in structure, but the two types differ in their genomic constituents. For instance, in addition to its role in gametogenesis (2), the X chromosome also plays an important role in neural differentiation, as indicated by X-linked mental retardation syndromes (3). These findings alluded to the significance and potential application of X-linked genes for studies on both neuronal lineages and tissue stem cells.

Brain-expressed X-linked (*BEX*) genes are a family of genes that reside on the mammalian X chromosome and show sequence similarity with transcription elongation factor A (SII)-like (*TCEAL*) genes. Although the molecular properties of *TCEAL* genes are obscure, a closely related protein, TFIIS/TCEA, maintains transcriptional fidelity by regulating the 3′-endoribonuclease activity of RNA polymerase II to bypass transcriptional pauses during the elongation process (4, 5). At least five members of the *BEX* family have been identified to date, including *BEX1*, *BEX2*, *BEX3*, *BEX4*, and *BEX5*, but *BEX5* appears to be lost in rodents (6). Members of this gene family were identified by screening of genes that are highly expressed in parthenogenic blastocysts (7) and account for more than 12% of the expressed sequence tags in the rat brain (6). In addition, these genes interact with olfactory marker proteins and are suggested to play an important role in olfactory neuronal development (8–10). Deregulated expression of this gene family has been related to human cancers; for instance, *BEX1* is a marker of neuroendocrine tumors (11). *BEX2* is also highly expressed in a subset of primary breast cancer cells (12) and gliomas (13)

* This work was supported in part by a grant-in-aid for scientific research on innovative areas from the Ministry of Education, Culture, Sports, and Technology, Japan.
[1] To whom correspondence should be addressed: Laboratory of Stem Cell Therapy, Tokai University Institute of Innovative Science and Technology, 143 Shimokasuya, Isehara, Kanagawa 259-1193, Japan. Tel.: 81-463-93-1121 (Ext. 2783); Fax: 81-463-95-3522; E-mail: kamiyaa@tokai-u.jp.

and regulates cell proliferation and survival by mediating nuclear factor-κB and c-Jun activity. In addition, *BEX2* is a marker for acute myeloid leukemia with a chromosomal translocation at the mixed lineage leukemia gene locus (14). Moreover, members of this gene family mediate nerve growth factor signaling (15–17) and possess a nuclear localization signal for their translocation to the nucleus (6, 15). Based on these reports, the *BEX* family genes are thought to function not only in cancer cells but also in developmental processes linking extracellular signaling to nuclear transcription events.

Although there are few studies on the physiological role of this gene family *in vivo*, recent studies using *Bex1* knock-out mice revealed that *Bex1* is involved in the regeneration of skeletal muscle (18) and neurons (19). Nonetheless, these mice displayed normal development and fertility, suggesting that other *Bex* genes play a redundant or major role in development. However, the functions of the other *Bex* family genes *in vivo* are not well known. In addition, although the expression of these genes has been examined through a screen of a cDNA library panel of bulk tissue samples (6), detailed analyses of their expression patterns at the cellular level have been difficult because of the challenges associated in raising specific antibodies against individual Bex family proteins. In this study, we investigated the expression of the *Bex* family genes in various tissues during the embryonic and adult stages. The results clearly showed that *Bex2* expression highly correlates with the development of hepatic progenitor cells. To determine the physiological function and the expression pattern of *Bex2* at the cellular level, we generated *Bex2*-deficient mice using a gene-targeting strategy by replacing the entire open reading frame (ORF) with enhanced green fluorescent protein (EGFP).[2] Molecular and cellular analyses of these mice revealed the significance and potential application of *Bex2* for future studies of endocrine and tissue stem/progenitor cells.

EXPERIMENTAL PROCEDURES

Materials—C57BL/6NCr mice, CAG-GFP transgenic mice, and ICR mice were purchased from Nihon SLC (Shizuoka, Japan). Animal experiments were performed with the approval of the Institutional Animal Care and Use Committee of both the Institute of Medical Science, University of Tokyo, and Tokai University. Dulbecco's modified Eagle's medium (DMEM), DMEM/Ham's F-12 half-medium, bovine serum albumin, penicillin/streptomycin/L-glutamine, dexamethasone, nicotinamide, 4,6-diamidine-2-phenylindole dihydrochloride (DAPI), 0.05% trypsin/EDTA, G418, and gelatin were purchased from Sigma. Insulin/transferrin/selenium X, nonessential amino acid solution, β-mercaptoethanol, and HEPES buffer solution were purchased from Invitrogen. Fetal bovine serum (FBS) was purchased from Nichirei Biosciences (Tokyo, Japan). Mitomycin C was purchased from Wako Pure Chemical (Osaka, Japan). PD0329501 and CHIR99021 were purchased from Axon Biochemicals (Groningen, The Netherlands).

Preparation of Mouse Embryonic Fibroblasts (MEFs)—At embryonic day (E) 12.5, ICR mouse embryos were dissected, and the head and internal organs were completely removed. The torso was minced and dissociated in 0.05% trypsin/EDTA for 30 min. After washing, cells were cultured in DMEM supplemented with 10% FBS and 1% penicillin/streptomycin/L-glutamine. MEFs were treated with mitomycin C at 37 °C for 2 h and used as feeder cells.

TABLE 1
Primers used for *Bex2* mouse genotyping and to generate probes for *Bex2-EGFP* knock-in ES Southern blotting

Primer	Sequence (5′ to 3′)
***Bex2* mouse genotyping**	
Bex2 forward (common)	cggtgctgaatctttgaaca
Bex2 reverse 1 (WT Exon3)	tgtctcacatcatccccaaa
Bex2 reverse 2 (EGFP)	ggtcttgtagttgccgtcgt
Sry forward	tcatgagactgccaaccacag
Sry reverse	catgaccaccaccaccaccaa
***Bex2-EGFP* knock-in ES Southern blotting**	
5′-Arm probe forward	aaaccattctttaattaaag
5′-Arm probe reverse	ttagcttactgtttactgagaa
3′-Arm probe forward	caaaacagaatgttggtttt
3′-Arm probe reverse	tcaaacgaatatttttattac

Embryonic Stem (ES) Cell Cultures and Gene Targeting—EGR-101 cells, ES cells derived from the C57BL/6 NCr mouse strain, were cultured on MEFs in M15G medium. M15G medium is a mixture of knock-out DMEM (Invitrogen) supplemented with 15% FBS, 1% penicillin/streptomycin/L-glutamine, β-mercaptoethanol (100 μM), and 1000 units/ml leukemia inhibitory factor (LIF; Chemicon, Temecula, CA). For gene targeting, plasmids carrying an EGFP-PGK-Neo-DTA cassette were used. Both the 7.8-kb region upstream of the third exon of *Bex2* (5′-homology arm) and the 2.8-kb region downstream of the third exon of *Bex2* (3′-homology arm) were cloned from BAC vectors containing a region that covered this genomic locus (clone Rp23-149K3; Geno Techs, Japan). The fragments were subcloned into the targeting vector. Purified plasmids were linearized with the AscI restriction enzyme and subsequently used for electroporation. One day after electroporation, transfected ES cells were selected with G418 (300 ng/ml) in culture. G418-resistant clones were expanded and genotyped over the short arm to detect the correct recombination by PCR. Selected clones were assayed again for correct recombination using Southern hybridization. For Southern hybridization probes, short fragments of Bex2 genome DNA were amplified using PCR and subcloned to pGEM-T easy vector System 1 (Promega, Madison, WI). PCR primers for mouse genotyping and the primers used for Southern hybridization probe generation are shown in Table 1.

Messenger RNA (mRNA) Detection by Reverse Transcription (RT)-PCR—Total RNA was extracted from primary and cultured cells using the RNeasy micro kit (Qiagen, Venlo, The Netherlands) or TRIzol (Invitrogen), according to the manufacturer's instructions. First-strand cDNA was synthesized using the High Capacity cDNA reverse transcription kit (Applied Biosystems, Foster City, CA) and used as a template for quantitative PCR. The cDNA samples were normalized by expression of glyceraldehyde 3-phosphate dehydrogenase (GAPDH), using the TaqMan probe (Applied Biosystems). Quantitative analyses of target mRNA expression levels were performed using the Universal Probe Library System (Roche Diagnostics). Primers and probes for both nonquantitative PCR and quantitative PCR are shown in Table 2.

[2] The abbreviations used are: EGFP, enhanced green fluorescent protein; MEF, mouse embryonic fibroblast; ChgA, chromogranin A.

TABLE 2

Primers and probes used for RT-PCR studies

The following abbreviations are used: *Bex*, brain-expressed X-linked; *Sox,* Sry-related box-containing; *Fox*, Forkhead box transcription factor; *Prdm14*, PR-domain containing 14; *Afp*, α-fetoprotein; *Cyp7a1*, cytochrome P450 family 7a1; *Hnf4α1*, hepatocyte nuclear factor 4A isoform 1; *Lgr5*, leucine-rich G protein-coupled receptor 5; *ChgA*, chromogranin A.

Gene	Forward (5′ to 3′)	Reverse (5′ to 3′)	Probe no.
qPCR (Roche Diagnostics universal probe library)			
Bex1	aggagaaggcaaggataggc	ttctgatggtatcttgtggcttt	63
Bex2	actacgccgcaagggatag	tttcacgccttgttccactt	2
Bex3	tgcccctaacttccgatg	catctccatctccacccaac	96
Bex4	actttctctgggccatacca	cttgacttctgttccctgcac	55
Nanog	ttcttgcttacaagggtctgc	agaggaagggcgaggaga	110
Sox2	ggcagagaagagagtgtttgc	tcttctttctcccagcccta	34
Prdm14	ggccataccagtgcgtgta	tgctgtctgatgtgtgttcg	16
Afp	catgctgcaaagctgacaa	ctttgcaatggatgctctctt	63
Foxa3	gcagtgcttccgggtatg	cctttgccatctcttttcca	81
Albumin	tgacccagtgttgtgcagag	ttctccttcacaccatcaagc	27
Cyp7a1	tctcaagcaaacaccattcct	ggctgctttcattgcttca	50
Hnf4α1	aaatgtgcaggtgttgacca	cgaggctccgtagtgtttg	64
Cytokeratin19	tgacctggagatgcagattg	cctcagggcagtaatttcctc	17
Osteopontin	ggaaaccagccaaggtaagc	tgccaatctcatggtcgtag	2
Sox17	cacaacgcagagctaagcaa	cgcttctctgccaaggtc	97
Hhex	tcagaatcgccgagctaaat	ctgtccaacgcatccttttt	2
Foxa2	gagcagcaacatcaccacag	cgtaggccttgaggtccat	77
Lgr5	cttcactcggtgcagtgct	cagccagctaccaaataggtg	60
Sox9	gaaagaccaccccgattaca	tccgcttgtccgttcttc	69
ChgA	cgatccagaaagatgatggtc	cggaagcctctgtctttcc	58
RT-PCR			
Bex1	tggtggtgagcatctctagaaagag	tagaagctggtaacagggag	
Bex2	gcagcgggaattgacaggagga	gtacatctcaaacatgtaag	
Bex3	ataggcccaggaaaacgaag	gggaatgaccgaagtcaagg	
Bex4	gaggagaaggcaaggatagg	ccccacttgataagagcttgt	
Gapdh	cttcaccaccatggagaaggc	ggcatggactgtggtcatgag	

Isolation and Analysis of Foregut Endodermal Cells—The foregut endodermal cells can be identified based on *Foxa3* expression in the foregut endoderm at around E8.5–9.0 (20–22). Transgenic mice expressing Venus fluorescent protein under the control of a Foxa3-enhancer promoter sequence were generated by pronuclear injection. Induced pluripotent stem cell lines were established from fibroblasts derived from the *Foxa3*-promoter-*Venus* transgenic mice using a Dox-inducible Oct3/4-Klf4-Sox2-expressing lentivirus (23). These cell lines were injected into tetraploid embryos and subsequently implanted into a pseudopregnant mouse. Somite numbers (somite pairs 6–15) were counted to validate the developmental stages identical to E8.5–9.0. *Foxa3*-positive regions were detected in these mouse embryos using fluorescence microscopy (Fig. 2*A*). These embryos were soaked in 0.25% trypsin/EDTA solution for 10 min at 37 °C and then dissociated by pipetting. Cells were collected in a staining buffer (phosphate-buffered saline (PBS) with 3% FBS) and subsequently stained with anti-CD45-PE-Cy7, anti-Ter119-PE-Cy7 (eBioscience, San Diego), and anti-EpCAM-Alexa647 (clone G8.8, Santa Cruz Biotechnology, Dallas, TX) antibodies for 30 min. After washing out the remaining antibody with PBS, cells were resuspended in staining medium containing propidium iodide and then sorted using a MoFlo™ fluorescence-activated cell sorter (FACS) (DAKO, Glostrup, Denmark). Specificity of the EpCAM antibody was validated by comparing the staining pattern between Alexa647 conjugated EpCAM antibody and its rat-IgG2a isotype control (eBioscience) on WT E9.0 embryos (Fig. 2*B*).

Hepatoblast Isolation and Culture—Hepatoblast isolation was performed as described previously (24). Minced embryonic liver tissues from E13.5 mice were dissociated with a 0.05% collagenase solution. Dissociated liver cells were washed with a staining buffer and then incubated with antibodies against cell surface markers (shown in Table 3) for 60 min at 4 °C. After staining the dead cells with propidium iodide, the cells were analyzed and sorted using a MoFlo™ cell sorter. $CD45^-Ter119^-CD71^-Dlk1^+CD133^+$ cells derived from E13.5 livers were purified as hepatoblasts in this study. For microarray analyses, $CD45^-Ter119^-c\text{-}Kit^-Dlk1^+CD133^+$ cells were used as hepatoblasts. MEFs were plated in culture dishes at a density of 2×10^5 cells/well (12-well plates) or

TABLE 3

Antibodies used for flow cytometry

The following abbreviations are used: FITC, fluorescein isothiocyanate; PE, phycoerythrin; APC, allophycocyanin; Dlk1, Delta-like 1 homolog.

Antibody	Clone	Company	Labels used
CD45.2	104	Biolegend	PE-Cy7
Ter119	Ter119	eBioscience	PE-Cy7
CD71	R17217	Biolegend	PE-Cy7, FITC
CD133	13A4	eBioscience	APC
Dlk1	24-11	MBL	PE
PDGFRα	APA5	Biolegend	APC
PCLP1	10B9	MBL	PE
Flk1	Avas12a1	eBioscience	PE
CD3	145-2C11	Tonbo-Bioscience	Biotin, FITC
CD4	RM4-5	Biolegend	Biotin, PE
CD8	53-6.7	eBioscience	Biotin, APC
Nk1.1	PK136	BD Biosciences	FITC
CD90.2 (Thy1.2)	53-2.1	BD Biosciences	PE
Ly6G&C (Gr-1)	RB6-BC5	eBioscience	Biotin, PE
CD11b (Mac-1)	M1/70	Biolegend	Pacific Blue
CD45R	RA3–6B2	eBioscience	Biotin, PE-Cy7
CD127 (IL7-RA)	A7R34	Biolegend	Biotin
CD34	RAM34	eBioscience	Alexa700
CD117 (c-Kit)	2B8	eBioscience	APC, PE-Cy7
Ly6A/E (Sca-1)	D7	eBioscience	PE-Cy7
Streptavidin	eBioscience	APC-Cy7	
E-cadherin	DECMA-1	eBioscience	Alexa Fluor647
rat IgG_1	eBRG1	eBioscience	PE, APC
rat IgG_{2a}	RTK2758	Biolegend	APC

3.2×10^6 cells/dish (100-mm dishes) prior to the day of hepatoblast isolation. For gene expression analysis, hepatoblasts (2×10^4 cells) purified from GFP-transgenic mouse embryonic livers were plated onto mitomycin C-treated MEFs in a 100-mm culture dish. After 5 days of culture, GFP^+ hepatoblasts were purified using a flow cytometer and used for RNA preparation. For colony formation assays, hepatoblasts isolated from both wild-type and *Bex2-EGFP* knock-in mouse embryos were purified and plated onto MEF feeder cells in 12-well tissue culture dishes (200 cells/well). Cells were cultured for 7 days in the standard culture medium in the presence of 40 ng/ml hepatocyte growth factor and 20 ng/ml epidermal growth factor (PeproTech; Rocky Hill, NJ). The standard culture medium used was a 1:1 mixture of hepatocyte colony formation medium (DMEM/Ham's F-12 half-medium supplemented with 1× insulin/transferrin/selenium X, 10 mM nicotinamide, 10^{-7} M dexamethasone, 2.5 mM HEPES, 1× penicillin/streptomycin/L-glutamine, and 1× nonessential amino acid solution) and fresh DMEM supplemented with 10% FBS. To count colonies derived from individual single cells, we used the ArrayScan VTI HCS Reader (Thermo Scientific, Waltham, MA) after immunostaining.

Isolation of Hepatic, Endothelial, Mesenchymal, and Hematopoietic Cells from E13.5 Fetal Liver by Flow Cytometry—Fetal liver cell fractionation was performed according to the method we have described previously (24). Briefly, minced embryonic liver tissue from E13.5 mice was dissociated with a 0.05% collagenase solution. Dissociated liver cells were washed with a staining buffer and incubated with antibodies against suitable cell surface markers (Table 3) for 60 min at 4 °C. After incubation with propidium iodide (for staining dead cells), the cells were analyzed and sorted using a MoFlo™ cell sorter. $CD45^-Ter119^-CD71^-Dlk1^+PDGFR\alpha^-$ cells were purified as hepatoblasts. $CD45^-Ter119^-CD71^-Dlk1^{mid}PDGFR\alpha^+$ cells were purified as mesenchymal cells. $CD45^-Ter119^-CD71^-Dlk1^{mid}PCLP1^+$ cells were purified as mesothelial cells. $CD45^-Ter119^-CD71^-Dlk1^{mid}Flk1^+$ cells were purified as endothelial cells. $CD45^+$ or $Ter119^+$ or $CD71^+$ cells were purified as hematopoietic cells.

Adult Hepatocyte and Bile Duct Epithelial Cell Isolation—Hepatocytes were isolated from 7-week-old livers following a two-step collagenase digestion (25). Briefly, perfused liver tissues were subsequently dissociated with a 0.05% collagenase solution. The mature hepatocyte fraction was separated from nonparenchymal cells with three low-speed centrifugations ($50 \times g$, 1 min). Dead cell debris was removed by centrifugation in 50% Percoll solution (GE Healthcare).

Bile duct epithelial cells were purified from a nonparenchymal cell fraction by collecting the supernatant of three low-speed centrifugations ($50 \times g$, 1 min). Dead cell debris was removed by centrifugation in 25% Percoll solution (GE Healthcare). The cells were then stained for antibodies against CD45, Ter119, and EpCAM. $CD45^-Ter119^-EpCAM^+$ cells were sorted as bile duct epithelial cells using a MoFlo™ cell sorter. Antibodies used in this step are shown in Table 3.

Immunostaining—Cultured cells were fixed in 4% paraformaldehyde in PBS, washed three times with PBS, and permeabilized with 0.5% Triton/PBS for 10 min. After washing with PBS, the cells were incubated with 5% donkey serum (Millipore, Bedford, MA) in PBS for 1 h at room temperature and then with diluted primary antibodies (Table 4) overnight at 4 °C. After washing with PBS, cells were incubated for 1 h at room temperature with an anti-rabbit IgG-Alexa488 antibody, an anti-rabbit IgG-Alexa546 antibody, or an anti-goat IgG-Alexa546 antibody (Invitrogen). Cell nuclei were then stained with DAPI.

TABLE 4
Antibodies used for immunocytochemistry and immunohistochemistry

Antibody	Host species	Company	Dilutions used
GFP	Chicken	Invitrogen	1:500
ChgA	Rabbit	Immunostar	1:500
Somatostatin	Rabbit	Nichirei Bioscience	Prediluted
Glucagon	Rabbit	Nichirei Bioscience	Prediluted
Insulin	Rabbit	Cell Signaling Technology	1:500
Albumin	Goat	Bethyl	1:750
CK19	Rabbit	Gift from Prof. Miyajima	1:3000
WT-1	Rabbit	Santa Cruz Biotechnology	1:100
Sox9	Rabbit	Millipore	1:100
Tra98	Rabbit	Bio academia	1:500
MVH	Rabbit	Abcam	1:100
PLZF	Rabbit	Santa Cruz Biotechnology	1:100
E-cadherin	Rabbit	eBioscience	1:250

For immunohistochemistry, paraffin-embedded sections were washed three times with xylene for 5 min and subsequently dehydrated by soaking the sections sequentially into 100, 90, 80, and 70% ethanol for 3 min. These samples were then autoclaved in Tris/EDTA solution (pH 9.0) for 15 min at 105 °C for antigen retrieval. The samples were then cooled at room temperature for more than 30 min. Then samples were washed with PBS, incubated with 5% donkey serum in PBS for 1 h at room temperature, and incubated with diluted primary antibodies (Table 4) overnight at 4 °C. After washing with PBS, sections were incubated for 1 h at room temperature with either anti-rat IgG-Alexa546 antibody, anti-rat IgG-Alexa647 antibody, anti-rabbit IgG-Alexa488 antibody, anti-rabbit IgG-Alexa546 antibody, or anti-goat IgG-Alexa546 antibody (Invitrogen). Cell nuclei were then stained with DAPI. Fluorescent images were obtained with the Axio Observer Z1 fluorescent microscope (Zeiss), BX51 fluorescent microscope (Olympus Corp., Tokyo, Japan), and BZ-9000 fluorescent microscope (Keyence, Japan).

Flow Cytometric Analysis of Hematopoietic Cells Derived from $Bex2^{EGFP/Y}$ Mice—For bone marrow analysis, the femurs and tibias of 8–10-week-old male mice were prepared. The bone marrow was flushed out, and the cell number was counted. Cell suspensions were immunostained with the antibodies listed in Table 3. Briefly, cells were stained with biotinylated antibodies against lineage markers (CD3, CD4, CD8, CD127, B220, Ter119, and Gr-1) for 30 min on ice. After washing with PBS, the cells were then stained with fluorescently labeled antibodies against markers such as CD34, CD117 (c-Kit), and Ly6A/E (Sca-1). At the same time, lineage markers were stained with streptavidin-APC-Cy7. Cells were purified using either a MoFlo™ cell sorter or a FACS Aria II system (BD Biosciences).

For gene expression analysis of the *Bex* family genes across the hematopoietic lineages, cells derived from the bone marrow, thymus, and spleen were prepared by surgically dissecting the tissues from wild-type 8- to 10-week-old C57BL/6NCr

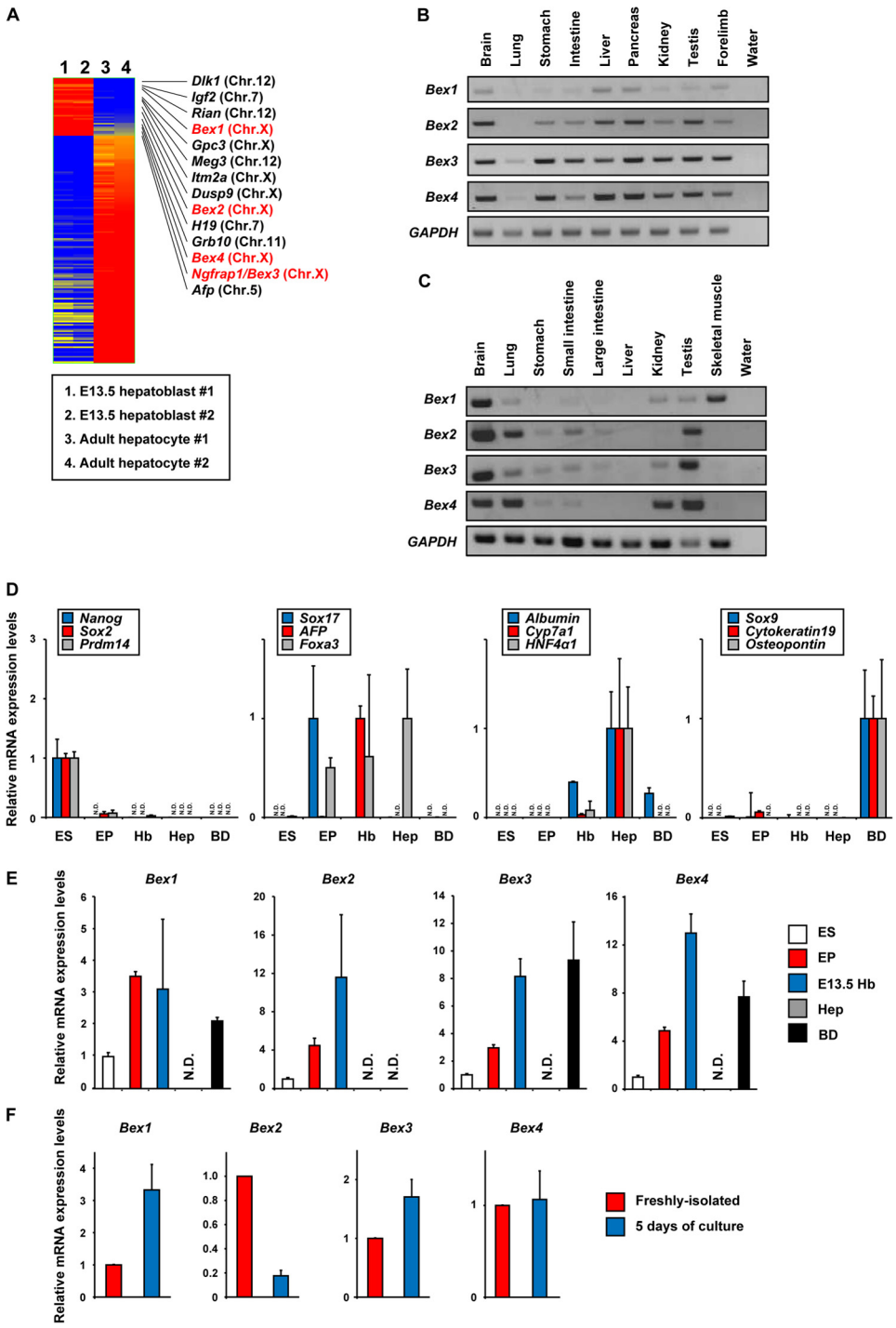

FIGURE 1. **Analysis of Bex family gene expression during development.** *A*, transcriptional profile during liver development. Gene expression in purified E13.5 hepatoblasts and adult hepatocytes was analyzed by microarray analysis ($n = 2$). Genes that showed differential expression by over 400-fold are shown. Several genes highly expressed in hepatoblasts are shown. *B* and *C*, Bex family gene expression in embryonic and adult tissues. Tissue samples of E13.5 (*B*) and 10-week-old (*C*) mice were surgically dissected, and total RNA was subsequently extracted from each sample. RT-PCR analyses for *Bex1*, *-2*, *-3*, and *-4*, and *GAPDH* (an internal control) were performed. *D*, expression of reference genes associated with ES cell (*Nanog*, *Sox2,* and *Prdm14*), endoderm cell (*Sox17* and *Foxa3*), hepatoblast (*Afp*), mature hepatocyte (*Albumin*, *Cyp7a1,* and *HNF4α1*), and bile duct epithelial cell (*Sox9*, *Cytokeratin19,* and *Osteopontin*). Cell fractions that represent the liver developmental path such as ES cells (*ES*), endodermal progenitor cells (*EP*), E13.5 hepatoblasts (*Hb*), mature hepatocytes (*Hep*), and bile duct epithelial cells (*BD*) purified from 7-week-old adult mice were used for quantitative PCR. The expression of the reference genes in the representative cell type was set at 1.0. Results are presented as the mean expression levels ± S.D. of samples, derived from three independent experiments. *N.D.* means not detected. Sampling procedures of endodermal progenitor cells are shown in Fig. 2. *E*, Bex family gene expression during endodermal and hepatic development. Relative Bex family gene expression levels in each cell fraction validated in *D* were analyzed using quantitative PCR. The expression in the ES cells was set at 1.0. Results are presented as the mean expression levels ± S.D. of samples, derived from three independent experiments. *N.D.* means not detected. *F*, Bex family gene expression in hepatoblast cultures. Relative Bex family gene expression levels in freshly isolated hepatoblasts and hepatoblasts after 5 days of culture were analyzed using quantitative PCR. The expression in freshly isolated hepatoblasts was set at 1.0. Results are presented as the mean expression levels ± S.D. of triplicate cultured samples.

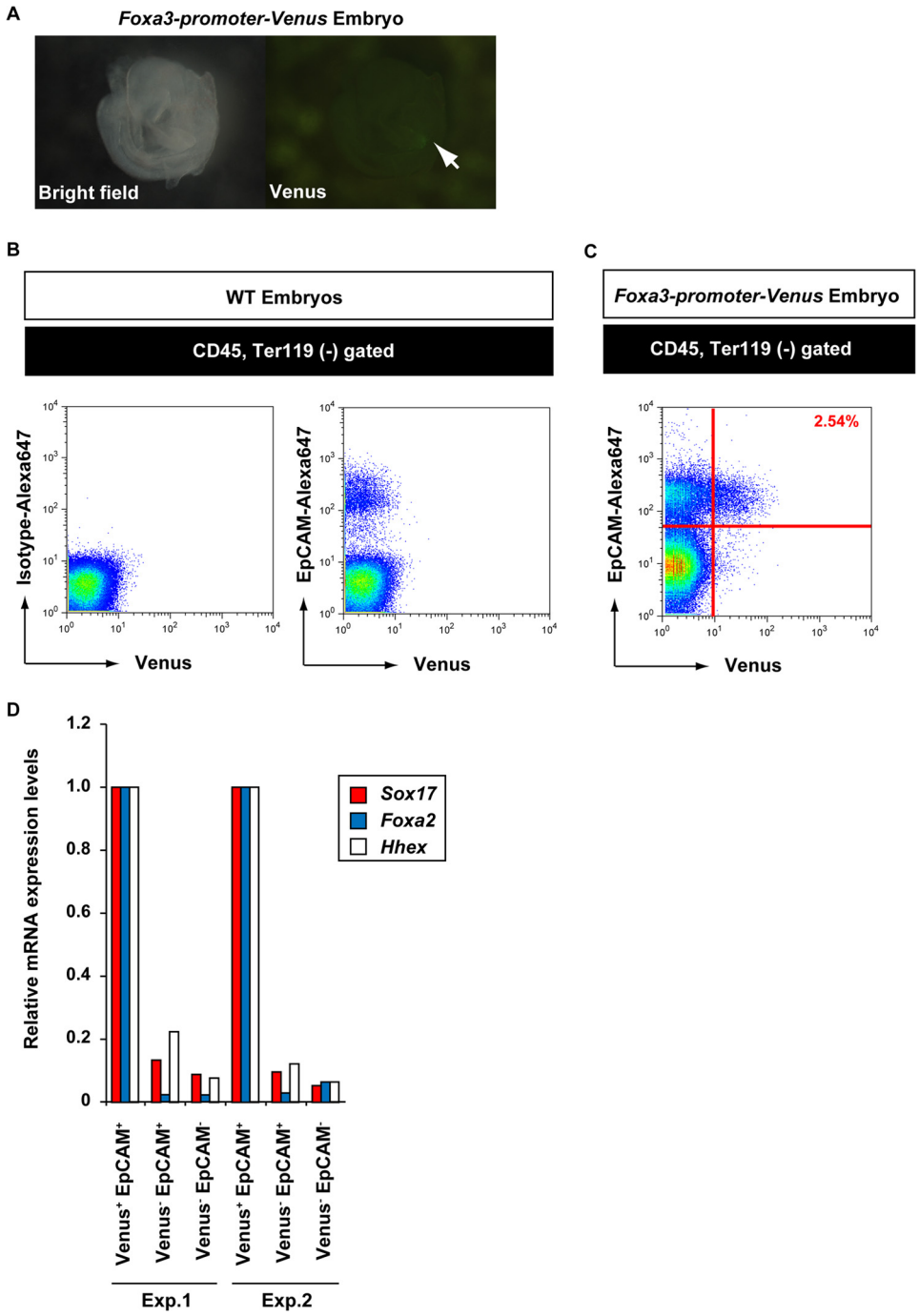

FIGURE 2. **Isolation of endodermal progenitor cells from *Foxa3*-promoter-*Venus* transgenic mice at E8.5–9.0.** *A*, mouse embryos generated from tetraploid injection of *Foxa3*-promoter-*Venus* transgenic iPS cells are shown. *Left*, bright field; *right*, Venus fluorescence. The *arrow* indicates Foxa3-Venus reporter activity in the hepatopancreatic endodermal region. Somite numbers from somite pairs 6–15 were counted to validate the developmental stages corresponding to E8.5–9.0. *B*, validation of the EpCAM antibody. Cell suspension derived from WT E9.0 embryos were stained for Alexa647-conjugated EpCAM antibody or its isotype (rat IgG2a) control. *C*, isolation of Venus$^+$EpCAM$^+$ cells from cell suspensions of E8.5–9.0 tetraploid embryos. A representative flow cytometry plot of the cell suspensions of E8.5–9.0 tetraploid embryos derived from *Foxa3*-promoter-*Venus* transgenic mice is shown. *D*, expression of the hepatopancreatic endoderm cell markers *Sox17*, *Foxa2*, and *Hhex* in purified cells from *C*. Relative expression levels of *Sox17*, *Foxa2*, and *Hhex* were analyzed by quantitative PCR. Expression levels of each gene in Venus$^+$EpCAM$^+$ cells are set at 1.0.

mice. Cells were stained with the antibodies listed in Table 3. Cells expressing each lineage marker or cells in the primitive fraction were sorted by a MoFlo^{TM} cell sorter.

Flow Cytometric Analysis of Stomach Samples from Bex2$^{EGFP/Y}$ Mice—For analyses of EGFP-positive cells in the pyloric stomach, stomach samples from 8- to 10-week-old *Bex2$^{EGFP/Y}$* mice were used. Stomachs of the *Bex2$^{EGFP/Y}$* mice were opened along the greater curvature, and the pyloric region was surgically isolated. After removal of the muscle layer by dissection, the epithelial layer was used for further analyses. The epithelial layer was minced in buffer containing EGTA for 3–5 h on ice and then dissociated by pipetting with a 10-ml pipette. The samples were then treated with 0.25% trypsin/EDTA (Sigma) for 30 min and then filtered through 45-μm

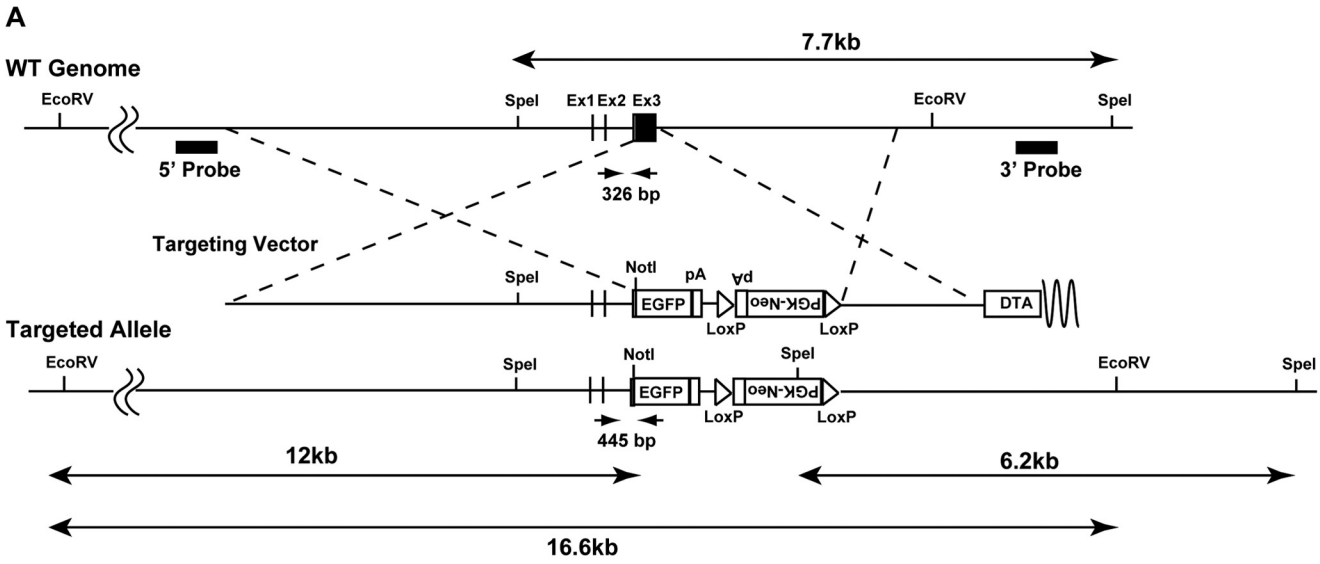

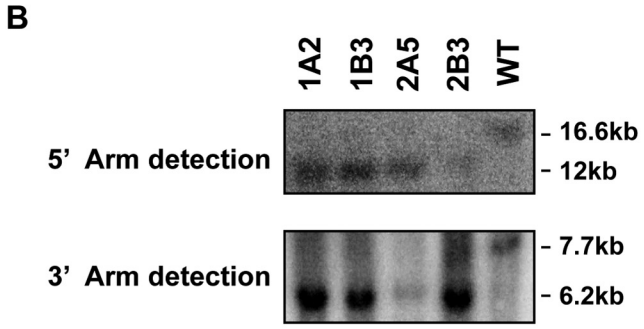

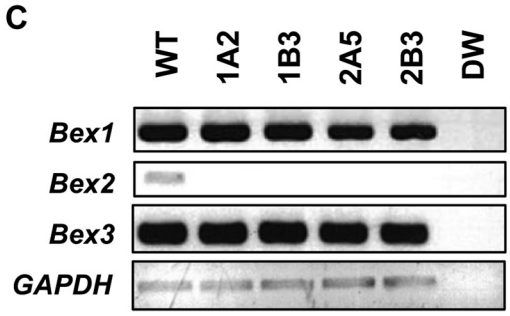

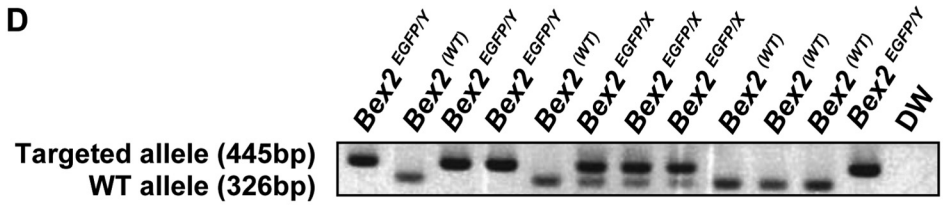

E

Mating results

Male	Female	Resulting genotype			
WT (C57BL6/NCr)	*Bex2* $^{EGFP/X}$	*Bex2*$^{EGFP/Y}$(38)	*Bex2*$^{EGFP/X}$(32)	*Bex2*$^{X/Y}$(27)	*Bex2*$^{X/X}$(16)
Bex2 $^{EGFP/Y}$	WT (C57BL6/NCr)		*Bex2*$^{EGFP/X}$(27)	*Bex2*$^{X/Y}$(10)	

FIGURE 3. **Generation of *Bex2* knock-out mice expressing an EGFP reporter by gene targeting.** *A*, targeting strategy for the *Bex2* genomic locus. Both the 7.8-kb upstream and 2.8-kb downstream fragments of the third exon of *Bex2* were subcloned into the targeting vector as the 5′- and 3′-homology arms, respectively. Restriction enzymes used for Southern blotting are depicted (EcoRV and NotI for 5′-arm detection and SpeI for 3′-arm detection). Probes used for Southern blotting are also shown as the *thick bar*. Using these probes and restriction enzymes, the targeted allele can be detected in a 12-kb (5′-arm) and 6.2-kb (3′-arm) band, whereas the wild-type allele is detected at 16 kb (5′-arm) and 7.7 kb (3′-arm), respectively. *Arrows* represent the primers designed for mouse genotyping. *B*, Southern blotting of the 5′-arm and the 3′-arm. The correct homologous recombination was confirmed in several ES clones (1A2, 1B3, 2A5, and 2B3). The parental ES cell line (*WT*) was used as a control. *C*, detection of *Bex1*, *-2*, and *-3* transcripts in the targeted ES cells. The parental ES cell line (*WT*) was used as a control. *GAPDH* was the internal control. *Bex2* expression was undetectable in the targeted ES cells. *D*, examples of the genotyping bands observed with genomic PCR of tissue samples from offspring born by mating *Bex2*$^{EGFP/X}$ female mice with wild-type C57BL/6NCr male mice. Distilled water (DW) was used as a negative control. *E*, numbers and the resulting genotypes of the offspring from *Bex2* knock-out mice.

mesh filters for flow cytometry. Cells were sorted by a MoFlo^{TM} cell sorter, and fractionated samples were collected and used for gene expression analysis. The primers used in the assay are listed in Table 2.

Transcription Profile Analysis Using Microarray—CD45^{-} Ter119^{-}CD133^{+}Dlk^{+} hepatoblasts derived from E13.5 livers and adult hepatocytes were purified as described above. Total RNA was purified from these cells using the RNeasy micro kit, according to the manufacturer's instructions. Transcription profiles were analyzed using the Agilent Whole Mouse Genome Microarray 4 × 44K. The original data are available from the Gene Expression Omnibus (accession number GSE56734).

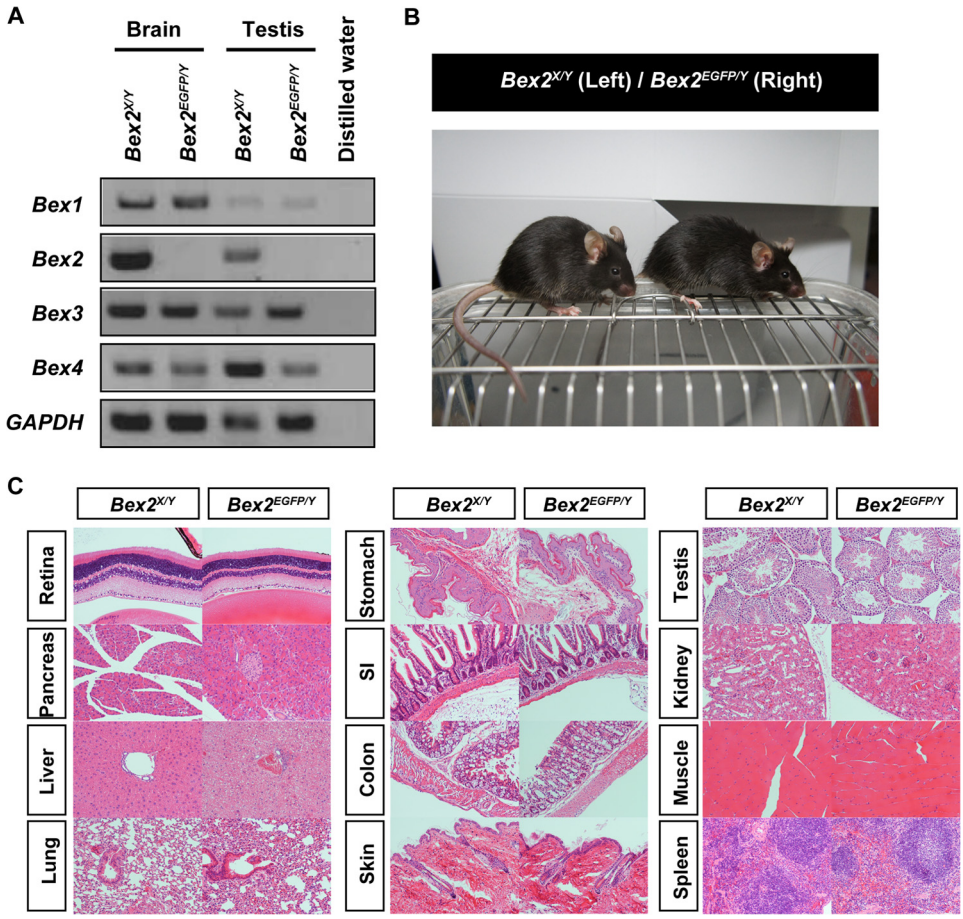

FIGURE 4. **Normal phenotypes of *Bex2* knock-out mice.** *A*, loss of *Bex2* mRNA in the brain and testis of *Bex2* knock-out mice. Total RNA was purified from the brain and testis of both wild-type (*Bex2*$^{X/Y}$) and knock-out (*Bex2*$^{EGFP/Y}$) mice. Bex family gene expression was analyzed using RT-PCR. *GAPDH* was the internal control. *B*, representative images of knock-out (*Bex2*$^{EGFP/Y}$) and littermate wild-type (*Bex2*$^{X/Y}$) mice. *Bex2*$^{EGFP/Y}$ mice grew into adults with normal appearances. *C*, hematoxylin and eosin staining of tissue sections from both wild-type (*Bex2*$^{X/Y}$) and knock-out (*Bex2*$^{EGFP/Y}$) mice. *SI,* small intestine.

Expression data were analyzed using Gene Springs 12.6. Datasets were normalized, and genes differentially expressed by more than 400-fold between the average of two groups (hepatoblasts *versus* adult hepatocytes) were extracted and represented as a heat map.

Statistical Analysis—Microsoft Excel 2007 (Microsoft, Redmond, WA) was used to calculate standard deviations (S.D.), and statistically significant differences between samples were determined by using a Student's two-tailed *t* test.

RESULTS

Bex2 Is Expressed in Stem/Progenitor Cell Populations during Liver Development—To identify genes that are specifically expressed in stem/progenitor cells, we performed comparative gene expression analysis between hepatoblasts (fetal hepatic stem/progenitor cells) and adult hepatocytes (Fig. 1*A*). Among the list of 30 genes that were more highly expressed in hepatoblasts by more than 400-fold compared with adult hepatocytes, the immature hepatocyte marker α-fetoprotein (*Afp*) as well as several genomic imprinted genes (*Dlk1*, *Igf2*, *H19*, *Grb10*, *Rian*, and *Meg3*) were identified. In addition to these genes, seven X-linked genes, including all the members of the *Bex* family genes, were also identified in the same list. Based on these data, we focused specifically on *Bex* family genes.

To gain insight into *Bex* family gene expression patterns in both embryonic and adult mice, we generated a tissue-specific cDNA panel from E13.5 and 10-week-old male mice. Subsequent RT-PCR analysis revealed the broad tissue expression of *Bex* family genes in the stage of embryonic development (Fig. 1*B*). Expression of these genes persisted at a high level in the brain and testis of adult mice. However, this expression was decreased in other tissues such as the endodermal organs and kidneys (Fig. 1*C*). Given that *Bex1*, *-2*, and *-3* are highly expressed in proliferating neural precursor cells and are down-regulated as the cells differentiate (15), we hypothesized that *Bex* family members would be specifically expressed in embryonic precursor cells of other somatic tissues as well. To confirm this hypothesis, we examined liver development using ES cells, endodermal progenitor cells isolated from *Foxa3*-promoter-*Venus* transgenic embryos (Fig. 2, *A*–*D*), fetal hepatoblasts, adult hepatocytes, and bile duct epithelial cells. Both Foxa2 and Foxa3 are known to be endodermal marker genes in mouse embryos. However, Foxa2 is also expressed in the cells of the notochord and the floor plate of the neural tube as well (26–28). In contrast, Foxa3 is mainly expressed in the endodermal cells at around E8.0-E.9.5 (21, 22, 29). We therefore have selected Foxa3 as an alternative marker to specifically detect the endo-

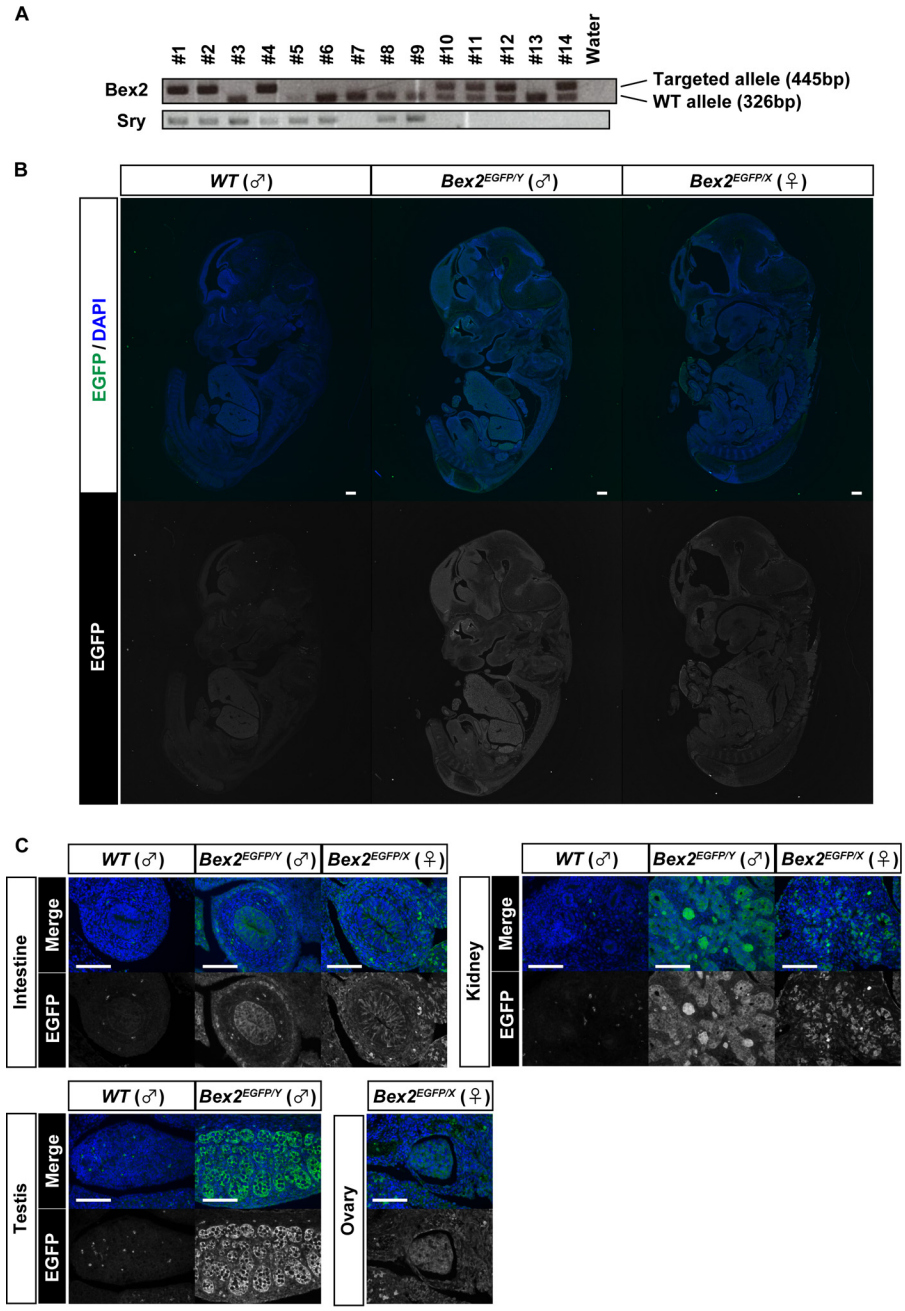

FIGURE 5. **Images of *Bex2* mutant fetuses at E13.5.** *A*, offspring born by mating of $Bex2^{EGFP/X}$ female mice with wild-type male mice. *Sry* was used to confirm male mice. $Bex2^{EGFP/Y}$ males and $Bex2^{X/Y}$ males were born in an expected Mendelian ratio. *B*, EGFP immunofluorescence in the embryos of wild-type male (*WT*, $Bex2^{X/Y}$), knock-out male ($Bex2^{EGFP/Y}$), and heterozygous female ($Bex2^{EGFP/X}$) at E13.5. Cell nuclei were stained with DAPI. *Scale bar* = 300 μm. *C*, magnified view of the immunofluorescence of EGFP in the intestine, kidney, and genital ridge (testis and ovary) of wild-type male (*WT*, $Bex2^{X/Y}$), knock-out male ($Bex2^{EGFP/Y}$), and heterozygous female ($Bex2^{EGFP/X}$) mouse embryos at E13.5. *Scale bar,* 100 μm.

dermal progenitor cells in the embryo. After confirming the expression pattern of reference genes (*Nanog*, *Sox2,* and *Prdm14* for ES cells; *Sox17* and *Foxa3* for endoderm; *Afp* for hepatoblasts, *Albumin*, *Cyp7a1,* and *HNF4α1* for hepatocytes; and *Sox9*, *Cytokeratin19,* and *Osteopontin* for ductal cells) (Fig. 1*D*), we found that *Bex* gene family expression increased during the ES cell and hepatoblast stages, but eventually it became undetectable in adult hepatocytes. Additionally, although the expression of *Bex1*, *-3*, and -4 was detectable at high levels, expression of Bex2 was below detectable levels in the bile duct epithelial cells (Fig. 1*E*).

In addition, we analyzed the expression of *Bex* family genes during the *in vitro* culture of fetal hepatoblasts. Recently, we established a colony formation culture using mesenchymal cells as feeder cells (30), which expands and differentiates fetal hepatoblasts into cells positive for albumin, a hepatocytic marker, or cytokeratin 19, a cholangiocytic and progenitor marker. Using this culture system, we found that among the *Bex* family genes, only *Bex2* was markedly decreased during this culture period, suggesting a correlation between the primary hepatic stem/progenitor-like state and *Bex2* expression (Fig. 1*F*). These results suggest

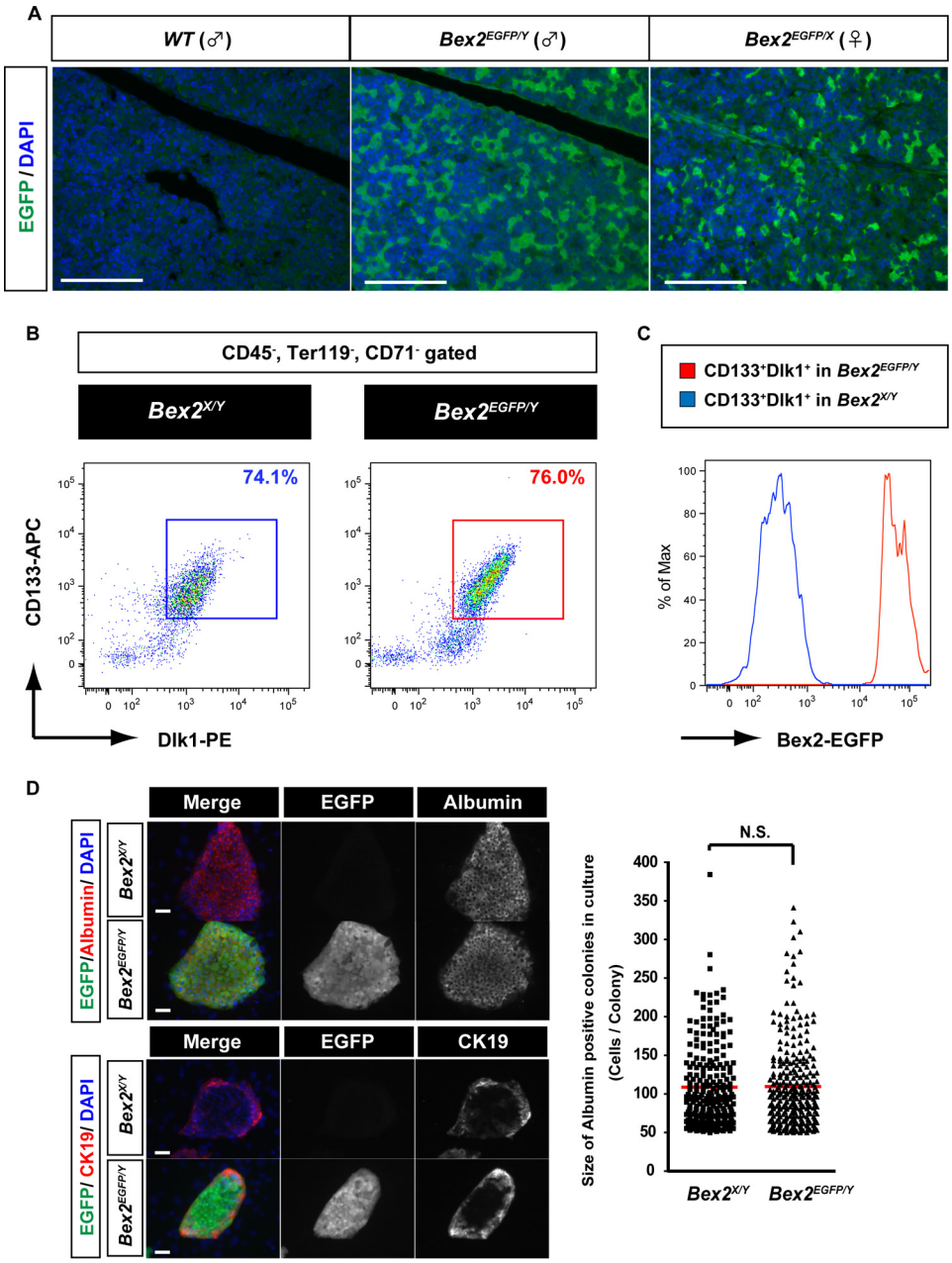

FIGURE 6. **Analyses of E13.5 hepatoblasts in Bex2 knock-out mice with the EGFP reporter.** *A*, representative immunohistochemical images of E13.5 embryonic livers derived from wild-type male mice (*WT*, $Bex2^{X/Y}$), knock-out male mice ($Bex2^{EGFP/Y}$), and heterozygous female mice ($Bex2^{EGFP/X}$). *EGFP* reporter expression controlled by the *Bex2* locus is shown. Cell nuclei were stained with DAPI. *Scale bar*, 100 μm. *B*, flow cytometry analysis of hepatoblast populations derived from both wild-type ($Bex2^{X/Y}$) and $Bex2^{EGFP/Y}$ mice. The proportions of $CD133^+Dlk1^+$ hepatoblasts in the nonhematopoietic cell fraction derived from E13.5 fetal livers are shown. *C*, EGFP expression in the $CD133^+Dlk1^+$ hepatoblast fraction from both wild-type and knock-out mice. Gates used for flow cytometry analyses are shown in *B*. *D*, analyses of the colony forming ability of hepatoblasts derived from wild-type ($Bex2^{X/Y}$) and $Bex2^{EGFP/Y}$ mouse livers. *Left*, representative immunocytochemical staining of the colonies derived from $CD133^+Dlk1^+$ hepatoblasts. Sorted cells were cultured for 7 days and stained with anti-albumin and cytokeratin 19 (*CK19*) antibodies. Note that the cells sorted from both genotypes formed colonies with albumin expression located in the central part of the colonies and cytokeratin 19 expression at the periphery. *Scale bars*, 100 μm. *Right*, numbers and sizes of the albumin-positive colonies formed in culture. The colony forming efficiency did not differ between the two groups. Representative data of colony formation in triplicate wells are shown. *N.S.* means not significant.

that *Bex2* is a novel marker for stem/progenitor cells during liver development.

Generation of Bex2 Knock-out Mice with the EGFP Reporter—To examine the physiological functions of *Bex2* and monitor the transcriptional activity of the *Bex2* genomic locus *in vivo*, we used a gene-targeting strategy to replace the 3rd exonic sequence encoding the entire ORF with an *EGFP* sequence and confirmed the correct recombination by Southern hybridization (Fig. 3, *A* and *B*). We also confirmed the absence of *Bex2* mRNA transcripts in these ES cells using RT-PCR (Fig. 3*C*). Although disrupting an X-linked gene in a male ES cell line could have a potentially negative effect on development, because it directly generates a nullizygous situation, *Bex2*-targeted ES cells exhibited normal proliferation *in vitro*. After confirming the normal karyotype, we injected the targeted cells into ICR blastocysts and obtained chimeric mice. We then collected sperm from these chimeras and performed intracytoplasmic sperm-head injections

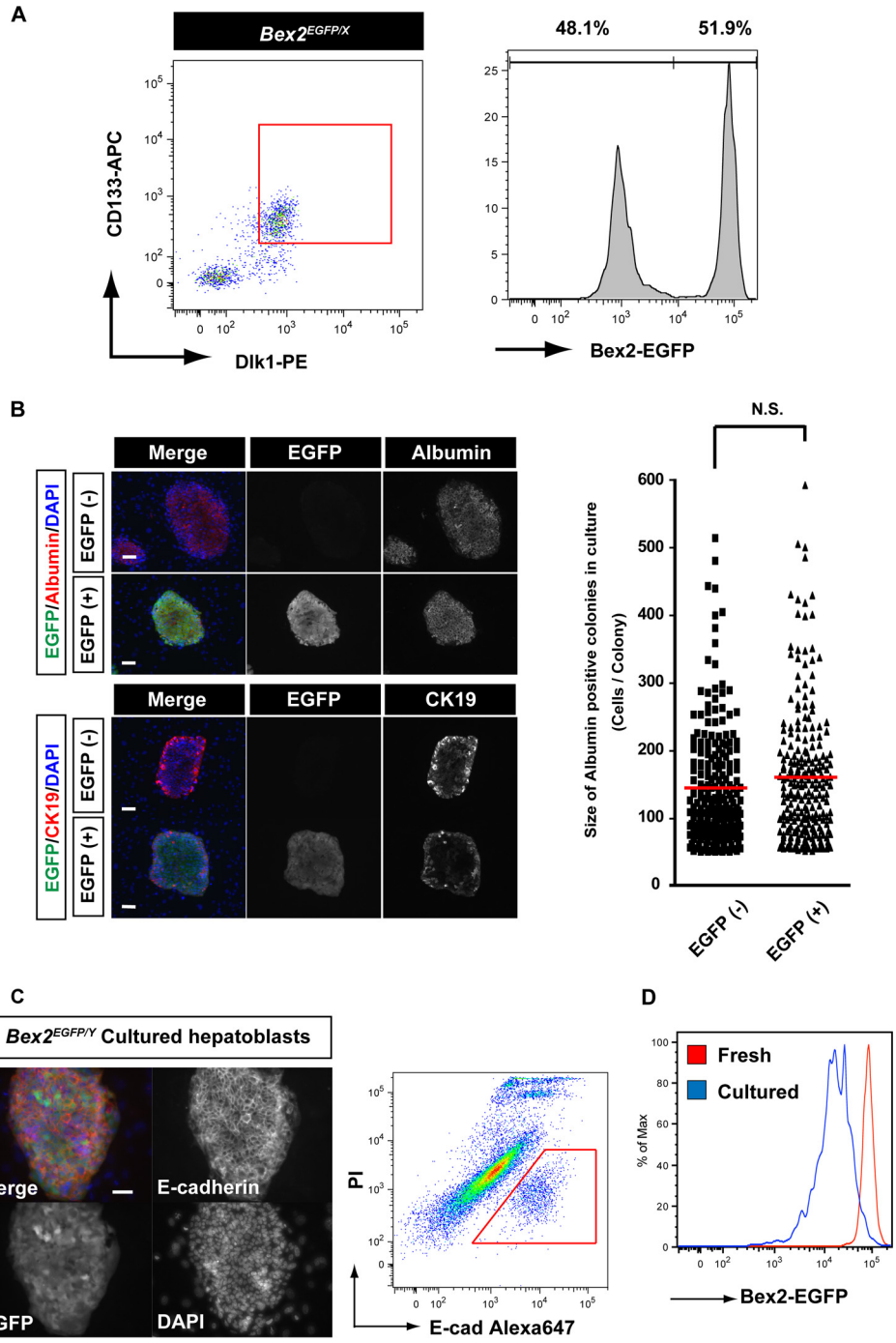

FIGURE 7. **Analysis of the *Bex2*$^{EGFP/X}$ fetal livers at E13.5.** *A*, flow cytometry analysis of the EGFP frequency in the hepatoblast fraction (CD45$^-$Ter119$^-$CD71$^-$CD133$^+$Dlk1$^+$, *red* gate) derived from the E13.5 *Bex2*$^{EGFP/X}$ fetal liver. The proportions of EGFP-positive and EGFP-negative cells are shown in the *histogram plot*. *B*, analysis of the colony forming ability of E13.5 hepatoblasts derived from either the EGFP-negative or EGFP-positive fraction of *Bex2*$^{EGFP/X}$ mouse livers. *Left*, representative immunocytochemical staining of the colonies derived from CD133$^+$Dlk1$^+$ hepatoblasts. Sorted cells were cultured for 7 days and stained with anti-albumin and cytokeratin 19 (*CK19*) antibodies. *Scale bars*, 100 μm. The cells sorted from both the EGFP-negative and EGFP-positive cell fractions formed colonies, with albumin expression in the center of the colonies and cytokeratin 19 expression at the periphery. *Right*, number and size of albumin-positive colonies formed in culture. The colony forming efficiency did not differ between the two groups. Representative data of colonies in triplicate wells are shown. *N.S.*, not significant. *C*, cultured hepatic cells express E-cadherin specifically, although feeder cells do not. Therefore, cultured hepatic cells can be resorted by flow cytometry based on E-cadherin expression. *Scale bars*, 50 μm. *D*, comparison of the Bex2^{EGFP} intensity between primary and cultured hepatoblasts. Bex2^{EGFP} intensity decreased during culture.

into host oocytes. Several female pups with the *Bex2*-targeted allele were born, suggesting that *Bex2*-deficient ES cells can contribute to the germ line and transmit their genome to the next generation.

Female mice with the targeted allele (*Bex2*$^{EGFP/X}$) were crossed with wild-type males. Healthy offspring carrying a targeted allele, both male (*Bex2*$^{EGFP/Y}$) and female (*Bex2*$^{EGFP/X}$), were born as shown in Fig. 3, *D* and *E*. Male offspring with no *Bex2* expression

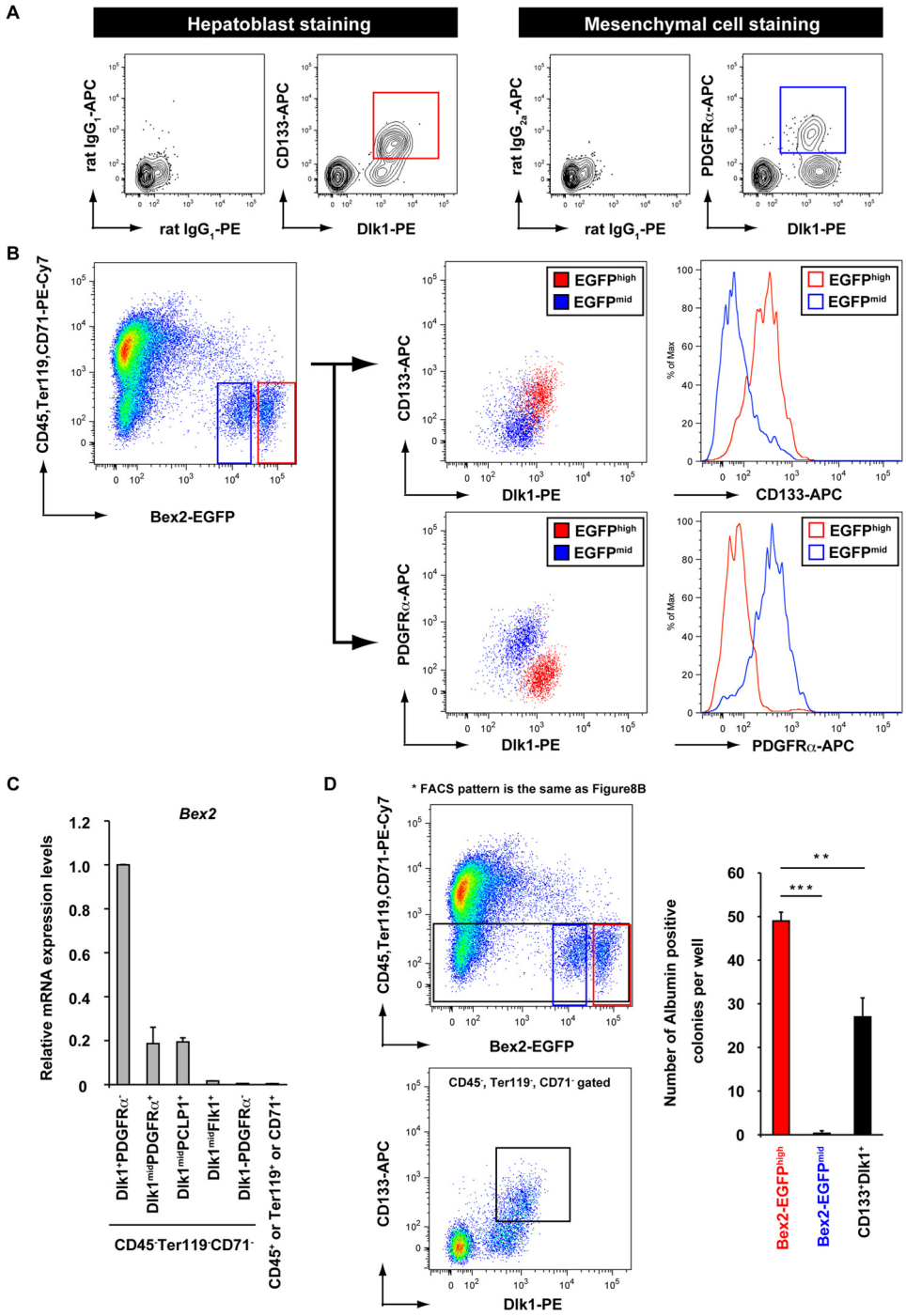

FIGURE 8. **Usage of Bex2-EGFP as a novel fetal liver hepatic progenitor marker.** *A,* staining pattern of hepatoblasts and mesenchymal cells derived from wild-type E13.5 fetal livers. CD45$^-$, Ter119$^-$, and CD71$^-$ negative cell fractions were stained with anti-Dlk1, CD133, and PDGFRα antibodies or their isotype control antibodies. *B,* flow cytometry analyses of Bex2$^{EGFP/Y}$ fetal liver cells. EGFP expression in the nonhematopoietic cell fraction is mainly consisting of two fractions, the EGFP^{high} fraction (gated in *red*) and the EGFP^{mid} fraction (gated in *blue*). In the *right panels*, both EGFP^{high} and EGFP^{mid} cell fractions gated in the *left panel* were analyzed using Dlk1, CD133, and PDGFRα antibodies. EGFP^{high} fraction cells are generally Dlk1$^+$CD133$^+$, although EGFP^{mid} fraction cells are mainly Dlk1^{mid}PDGFRα^+. *C,* expression of Bex2 transcript in fractionated fetal liver cells. Fetal liver cells from E13.5 livers were fractionated into cells enriched for hematopoietic cells (CD45$^+$ or Ter119$^+$ or CD71$^+$) or nonhematopoietic cells (CD45$^-$Ter119$^-$CD71$^-$ gated) such as hepatoblasts (Dlk1$^+$PDGFRα^-), mesenchymal cells (Dlk1^{mid}PDGFRα^+), mesothelial cells (Dlk1^{mid}PCLP1$^+$), endothelial cells (Dlk1^{mid}Flk1$^+$), and other uncharacterized cells (Dlk1$^-$PDGFRα^-). The expression of *Bex2* in the hepatoblasts (Dlk1$^+$PDGFRα^-) was set at 1.0. Results are presented as the mean expression levels ± S.D. of samples, derived from three independent experiments. *D,* comparison of the hepatic (albumin-positive) colony forming efficiency between EGFP^{high} fraction (gated in *red*), EGFP^{mid} fraction (gated in *blue*), and Dlk1$^+$CD133$^+$ fraction (gated in *black*) in the nonhematopoietic cells. Note that the flow cytometry pattern shown in the *upper-left panel* is the same as the one shown in *B* (**, $p < 0.05$; ***, $p < 0.0001$).

(*Bex2*$^{EGFP/Y}$) grew into adulthood (Fig. 4, *A* and *B*). Histological analysis of various tissues revealed that there were no differences between *Bex2*$^{EGFP/Y}$ adult males and wild-type *Bex2*$^{X/Y}$ littermates, at least at the macroscopic level (Fig. 4*C*).

Bex2 Serves as a Novel Marker of Hepatoblasts in the Mid-fetal Liver, but Its Loss Does Not Affect Proliferation and Differentiation—We crossed *Bex2*$^{EGFP/X}$ female mice with wild-type male mice and obtained two types of *Bex2* knock-in

embryos (*Bex2*$^{EGFP/Y}$ males and *Bex2*$^{EGFP/X}$ females) and control littermates (Fig. 5, *A* and *B*). Bex2 knock-in mice had specific EGFP signals in various organs such as intestine, genital ridge (testis for male and ovary for female), kidney (Fig. 5*C*), and liver (Fig. 6*A*). In particular, cells expressing EGFP at high levels were scattered in clusters in the fetal liver, resembling the structural localization of hepatoblasts. In all the tissues examined, the number of EGFP-positive cells in the *Bex2*$^{EGFP/X}$ female embryos was smaller than that of *Bex2*$^{EGFP/Y}$ male embryos in these tissues. The underlying mechanism to this phenomenon, if not all, might be the X chromosome inactivation occurring in the individual cells at the early pre-implantation embryo stage, which makes the female heterozygous *Bex2*$^{EGFP/X}$ mice a mosaic of cells that have either the activated or inactivated X chromosome. Based on our initial observation that Bex2 is highly expressed in fetal hepatoblasts and becomes down-regulated upon hepatic differentiation, we specifically focused on the phenotypes of Bex2-deficient hepatoblasts using an *in vitro* colony assay. *Bex2*-deficient fetal livers from *Bex2*$^{EGFP/Y}$ males showed normal cellular numbers and percentages of hepatoblasts (the CD133$^+$Dlk1$^+$ cells in the CD45$^-$Ter119$^-$CD71$^-$ nonhematopoietic cell fraction) compared with their wild-type *Bex2*$^{X/Y}$ male littermates (Fig. 6*B*). Hepatoblasts derived from *Bex2*$^{EGFP/Y}$ fetal livers were strongly positive for EGFP (Fig. 6*C*), indicating that the transcriptional activity of the *Bex2* locus is high in hepatoblasts. In addition, the colony forming ability of *Bex2*$^{EGFP/Y}$ hepatoblasts was similar to that of wild-type hepatoblasts (Fig. 6*D*).

Bex2$^{EGFP/X}$ mice have both Bex2$^+$ and Bex2$^-$ cells because of X chromosome inactivation at the early embryonic stage. If the targeted allele is on the inactivated chromosome, these cells are theoretically wild-type. However, if the targeted allele is on the active X chromosome, cells with active *Bex2* locus are EGFP-positive but *Bex2*-deficient. Taking advantage of this competitive situation, we analyzed the hepatoblasts in *Bex2*$^{EGFP/X}$ female fetal livers. The proportions of EGFP-positive cells and EGFP-negative cells in the hepatoblast fraction derived from *Bex2*$^{EGFP/X}$ livers were nearly equal (Fig. 7*A*), suggesting that loss of *Bex2* does not affect cell proliferation, even in a competitive situation during the mid-fetal stages. In addition, hepatoblasts isolated from either the EGFP-positive or EGFP-negative fraction formed colonies at similar levels (Fig. 7*B*).

In this culture system, hepatoblasts can be distinguished and isolated from MEFs by the expression of the epithelial cell marker E-cadherin (Fig. 7*C*). Therefore, we compared EGFP expression between freshly isolated hepatoblasts and 7-day-cultured hepatoblasts. Nearly a 10-fold (1-log) decrease in the EGFP intensity was detected in cultured hepatoblasts derived from *Bex2*$^{EGFP/Y}$ mice (Fig. 7*D*). These data confirm the mRNA expression data shown in Fig. 1*D*. These results suggested that the defect of *Bex2* in hepatoblasts is compensable both *in vitro* and *in vivo*, and the transcriptional activity of the *Bex2* locus in hepatoblasts can be monitored by EGFP fluorescence during liver development.

Finally, we assessed whether the activity of the EGFP reporter is useful for the purification of hepatoblasts in mouse fetal livers. E13.5 fetal liver contains various types of cells such as hepatoblasts, mesenchymal progenitor cells, mesothelial cells, endothelial cells, and hematopoietic cells. We have previously reported that hepatoblasts can be enriched by the expression of CD133 and Dlk1 (31), while mesenchymal cells can be sorted by the expression of lower levels of Dlk1 and a prominent expression of PDGFRα (Fig. 8*A*) (24). Using flow cytometry, we analyzed the EGFP reporter-active cells in the fetal liver of *Bex2*$^{EGFP/Y}$ mice. The higher EGFP reporter activity (Bex2-EGFP^{high}) was evident in the presumptive hepatoblast fraction expressing both CD133 and Dlk1 (Fig. 8*B*, *red cells*). However, the lower EGFP reporter activity (Bex2-EGFP^{mid}) was generally detected in the mesenchymal cell fraction expressing PDGFRα (Fig. 8*B*, *blue cells*). We confirmed these results by analyzing the expression levels of *Bex2* mRNA transcripts in wild-type E13.5 fetal liver cells using quantitative PCR. Expression levels of *Bex2* transcripts were the highest in the hepatoblast fraction, although lower expression levels of *Bex2* were also detected in both mesenchymal and mesothelial cell fractions (Fig. 8*C*).

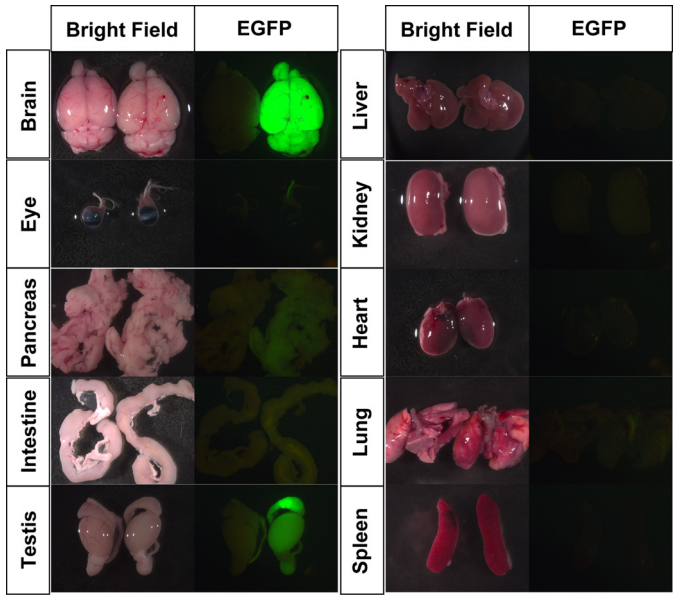

FIGURE 9. **Macroscopic view of tissues derived from *Bex2*$^{EGFP/Y}$ and wild-type littermate mice at 9 weeks old.** Macroscopic views of the brain, eye, pancreas, intestine, testis, liver, kidney, heart, lung, and spleen are shown. The bright field and EGFP fluorescence of both wild-type (*left*) and *Bex2*$^{EGFP/Y}$ (*right*) tissues are shown.

We also confirmed that Bex2-EGFP^{high} cells but not Bex2-EGFP^{mid} cells are hepatic progenitor cells that are capable of forming hepatic (albumin-positive) colonies *in vitro* (Fig. 8*D*). Interestingly, we compared the hepatic colony-forming efficiency between Bex2-EGFP^{high} cells and Dlk1$^+$CD133$^+$ cells and found that Bex2-EGFP^{high} cells give higher hepatic colony-forming efficiency. Dlk1 is known to be expressed in the mesenchymal cells (24, 32), and CD133 is expressed in a minor subset of mesenchymal cells similar to hepatoblasts. Therefore, Dlk1$^+$CD133$^+$ cells purified using flow cytometry technically harbor risks of contamination of mesenchymal cells at a certain frequency and thus result in lower sorting efficiency of hepatoblasts. These results suggest the potential utility of Bex2 as a novel specific marker for fetal hepatoblasts.

Expression Profiling of Bex2 Genomic Locus Transcriptional Activity in Adult Tissues—As mentioned above, we could not detect obvious phenotypes in *Bex2*-deficient mice, particularly

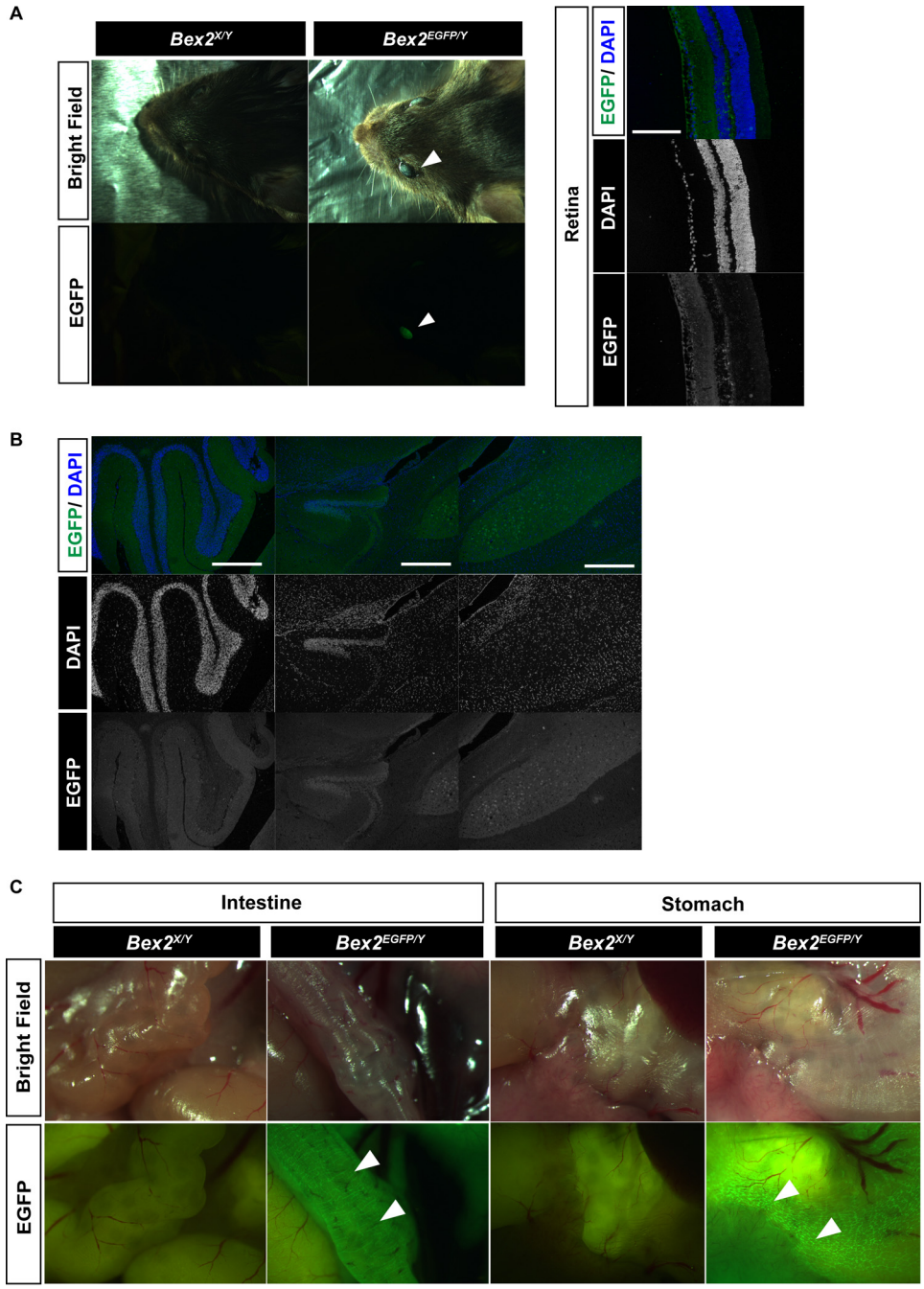

FIGURE 10. **Analysis of EGFP fluorescence in neuronal tissues.** *A*, macroscopic views of the heads of both wild-type (*Bex2*$^{X/Y}$) and *Bex2*$^{EGFP/Y}$ mice (*left*). *Arrowheads* indicate the EGFP signal specifically observed in the eye of *Bex2*$^{EGFP/Y}$ mice. Immunohistochemical analysis of EGFP in the retinal section of *Bex2*$^{EGFP/Y}$ mice showed activation of the *Bex2* locus in retinal neural cells (*right*). *B*, immunohistochemical analysis of EGFP expression across various regions of the brain. *Scale bars,* 100 μm. *C*, macroscopic views of the gastrointestinal tissues of wild-type (*Bex2*$^{X/Y}$) and *Bex2*$^{EGFP/Y}$ mice. A reticulated EGFP structure was observed at the surface of the intestine and in the stomach from *Bex2*$^{EGFP/Y}$ mice.

during liver development. However, these mice are useful for labeling hepatoblasts in the fetal liver using EGFP fluorescence. In addition, the EGFP intensity in adult mice was most evident in the brain and testis, although it was undetectable in the liver and kidney at macroscopic levels (Fig. 9). These results were consistent with the RT-PCR results using wild-type mouse tissues. This suggested that *Bex2* deficiency did not affect *Bex2* locus transcriptional activity, as monitored by EGFP. Thus, we aimed to obtain comprehensive information on the precise *Bex2* expression pattern in adult tissues at the cellular level using EGFP fluorescence as readout of endogenous *Bex2* genomic locus transcriptional activity.

Bex2-EGFP Reporter Is Active in the Central and Peripheral Neuronal Cells—Because the *Bex2* locus was significantly active in the brain and eye (Fig. 9), we analyzed the EGFP fluorescence pattern of eye and brain tissue section samples from *Bex2*$^{EGFP/Y}$ mice. EGFP fluorescence was positive in the entire neural retina and in the brain, suggesting that the *Bex2* locus is active in most of the regions in the retina and brain (Fig. 10, *A* and *B*). These results are consistent with previous reports (10). In addition,

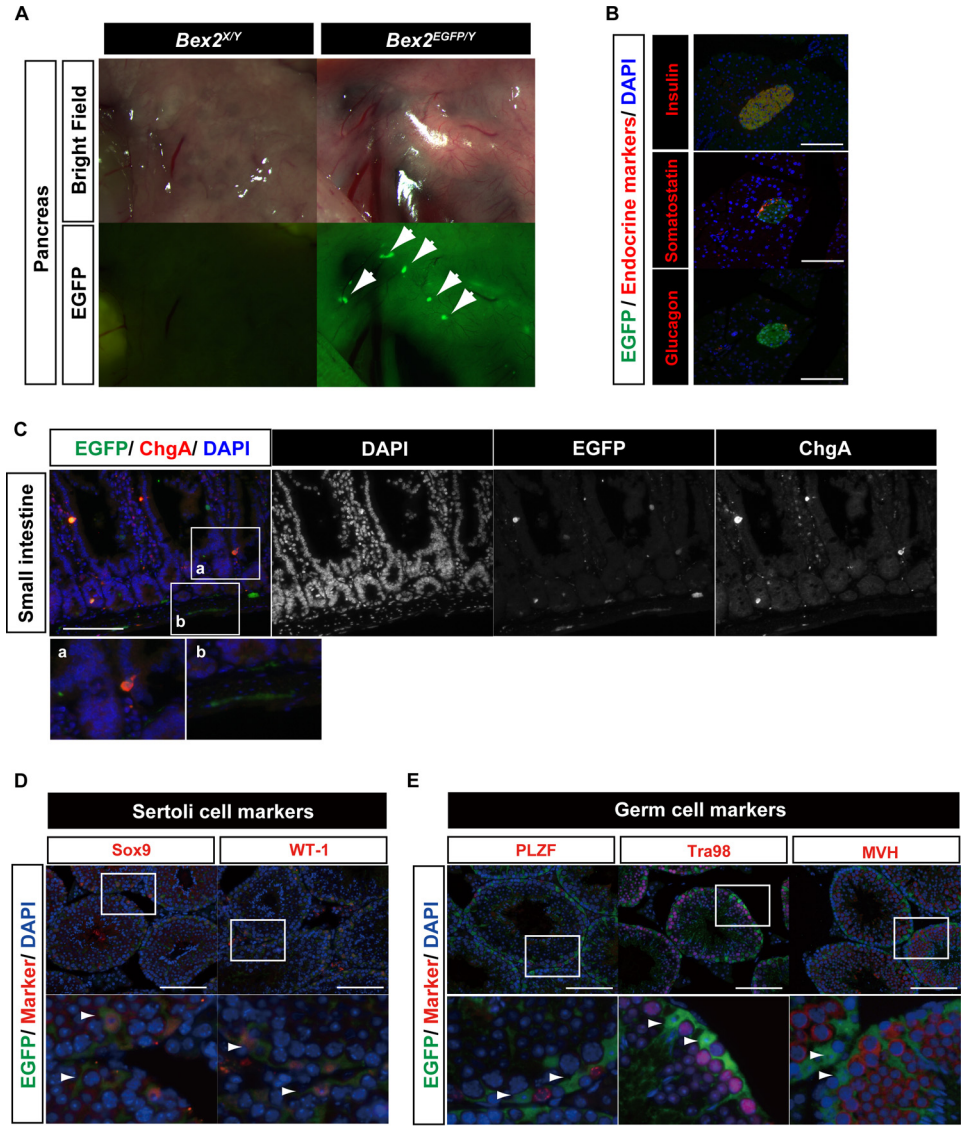

FIGURE 11. **Bex2-EGFP marks endocrine cells of the pancreas, intestine, and seminiferous tubules.** *A*, macroscopic views of EGFP fluorescence in the pancreatic islets derived from 9-week-old mice. *Arrowheads* indicate the presence of pancreatic islets. *B*, immunohistochemical analysis of pancreatic endocrine cell markers (*red* = insulin, somatostatin, or glucagon) in the pancreas. EGFP-bright cells merged with the three endocrine cell lineages. *C*, immunohistochemical analysis of intestinal endocrine cell markers (*red* = ChgA) in the intestinal epithelium. Intestinal epithelial EGFP-expressing cells are ChgA-expressing cells (*panel a*). EGFP-bright cells near the muscular layer do not express ChgA (*panel b*). *D*, immunohistochemical analysis of Sertoli cells. EGFP-positive cells expressed the Sertoli cell markers Sox9 and WT-1, shown by *arrowheads*. *E*, immunohistochemical analysis of germ cells in the testicular seminiferous tubules. EGFP fluorescence did not merge with the germ cell markers PLZF, Tra98, and MVH, shown by *arrowheads*. *Scale bars* = 100 μm.

EGFP-positive neuronal cells were observed on the surface of gastrointestinal tissues in a reticulated structure (Fig. 10*C*), suggesting that *Bex2* is active not only in the central nervous system but also in the peripheral nervous system.

Bex2-EGFP Reporter Is Active in Endocrine Cells—Endocrine cells of the digestive tract consist of pancreatic cells, clustered in the islets of Langerhans (33), and scattered cells, distributed throughout the digestive epithelium from the stomach to the colon (34), the latter of which are known as enteroendocrine cells. In the pancreas, basal EGFP intensity was observed, but the most evident EGFP signal appeared as a dotted structure (Fig. 11*A*). By immunohistochemistry, we confirmed that the bright EGFP intensity was derived from cells producing somatostatin (α-cells), insulin (β-cells), and glucagon (γ-cells) (Fig. 11*B*). Therefore, in the pancreas, *Bex2* seems to be a common marker for all endocrine cells. We next evaluated whether a *Bex2* signal could be observed in the endocrine cells of gastrointestinal tissues. Interestingly, EGFP was detected in cells expressing Chromogranin A (ChgA), a secretory protein generally produced by enteroendocrine cells in both the small intestine and colon (Fig. 11*C*, *panel a*). We also observed a strong EGFP-positive area at the submucosal region of the intestinal tube, a structure representing the neural lineage in the intestinal tissue (Fig. 11*C*, *panel b*). Therefore, we found that *Bex2* is not only a marker for the neural cell lineage but also for the endocrine cell lineage in gastrointestinal tissues. In the testis, the Sertoli cell is a major somatic cell type that plays a central role combining endocrine action and spermatogenesis (35, 36). In the $Bex2^{EGFP/Y}$ mice, EGFP expression was evident in the periphery of the seminiferous tubules. Both Sertoli cells

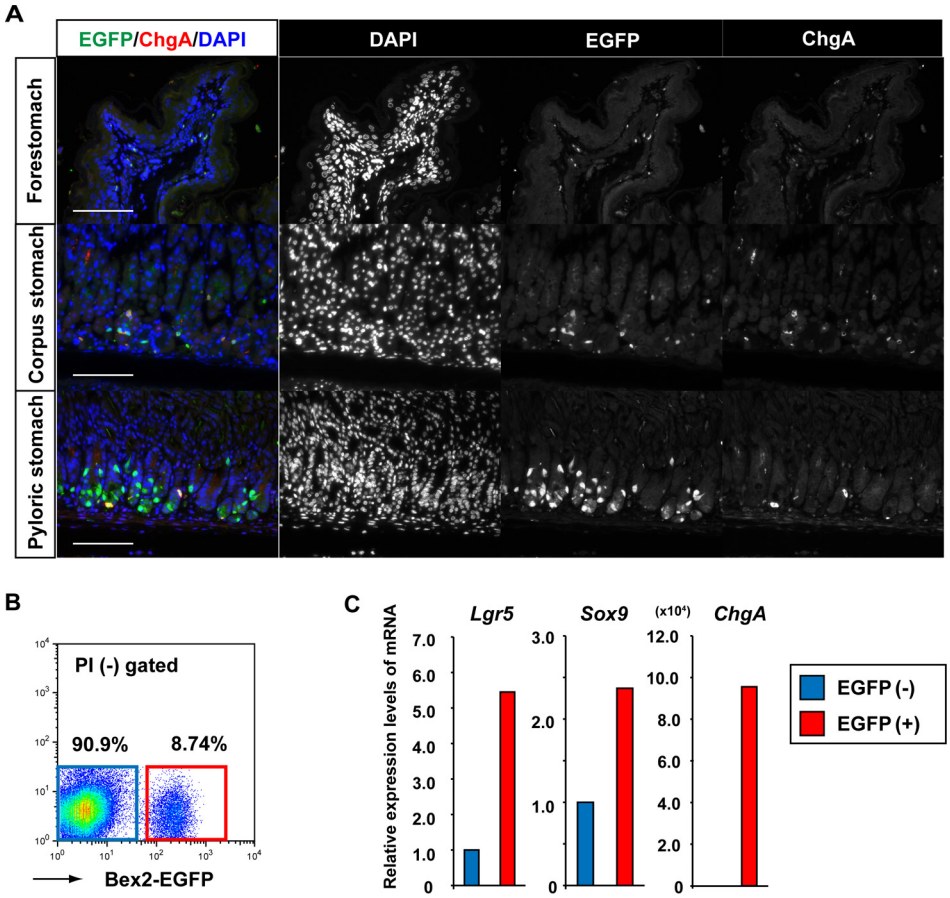

FIGURE 12. **Bex2-EGFP marks stem/progenitor cells in the pyloric stomach.** *A*, immunohistochemical analyses of ChgA in the forestomach, corpus, and pyloric regions of the stomach derived from *Bex2*$^{EGFP/Y}$ mice. *Scale bars,* 100 μm. *B*, flow cytometric analysis of EGFP-expressing cells in the pyloric region. *C*, quantitative PCR analyses for the stem cell markers *Lgr5* and *Sox9* in the pyloric stomach and for the endocrine cell marker *ChgA*. Results are presented as the mean values of a representative experiment with three technical replicates. Expression in the EGFP-negative fraction was set at 1.0. Sorting gates for these samples are shown in *B*.

and germ cells (spermatogonia) are enriched in the peripheral region of the testis. Therefore, we stained these cells using specific antibodies against Sertoli and germ cell markers. EGFP expression was detected in cells positive for both Sox9 and WT-1, Sertoli cell markers (Fig. 11*D*), but not in cells positive for MVH, Tra98, and PLZF, germ cell markers (Fig. 11*E*). These results suggest that the *Bex2* locus is specifically active in the Sertoli cells but not germ cells in the testis.

Bex2-EGFP Reporter Is Active in Stem/Progenitor Cells in the Pyloric Stomach and in Hematopoietic Lineages—Recent reports have shown that molecules such as *Lgr5* and *Pw1* are specifically expressed in stem cells among various tissues (37, 38). As shown above, *Bex2* expression correlated with stem/progenitor cell phenotypes in the fetal liver. Therefore, we hypothesized that *Bex2* might also be useful for marking stem/progenitor cells in other tissues. Through immunohistochemical analyses of various tissues, we found that EGFP-expressing cells were enriched at the bases of glands in the pyloric stomach, where rapidly proliferating *Lgr5*$^+$ stem cells were recently identified (39). As described above, a subset of these EGFP-positive cells were ChgA-expressing endocrine cells. However, many ChgA$^-$EGFP$^+$ cells were detected in this region (Fig. 12*A*). EGFP-positive cells were absent in the forestomach and were very rare in the corpus region. We also analyzed whether previously reported stem cell markers (39) are expressed in the EGFP-positive cell fraction isolated from the pyloric epithelium. In addition to *ChgA*, expression of *Lgr5* and *Sox9*, markers of pyloric epithelial stem cells, was enriched in the EGFP-positive cell fraction (Fig. 12, *B* and *C*), suggesting that *Bex2*-positive cells in the pyloric epithelium contained both a stem/progenitor cell fraction and an endocrine cell fraction.

Next, the EGFP-positive cell distribution along the hematopoietic cell lineage was analyzed. Using flow cytometry, we found that the c-Kit$^+$Sca-1$^+$Lineage$^-$ (KSL) cell fraction, which is known to be rich in hematopoietic stem/progenitor cells (40), contains EGFP-positive cells at a higher frequency than the more committed progenitor cells (Lineage$^-$ fraction). In addition, further enrichment for hematopoietic stem cells within the KSL fraction using CD34 expression (41) revealed that EGFP-positive cells were found in greater abundance in the CD34$^-$KSL stem cell fraction compared with the CD34$^+$KSL progenitor cell fraction (Fig. 13, *A* and *B*). To confirm that this was not an artificial observation in the genetically modified *Bex2*-deficient mice, *Bex* family gene expression was analyzed by quantitative PCR in several hematopoietic cell fractions derived from wild-type mice (Fig. 13*C*). The *Bex* family genes were most strongly expressed in CD34$^-$KSL cells. In contrast, lower levels of gene expression were detected in progenitor

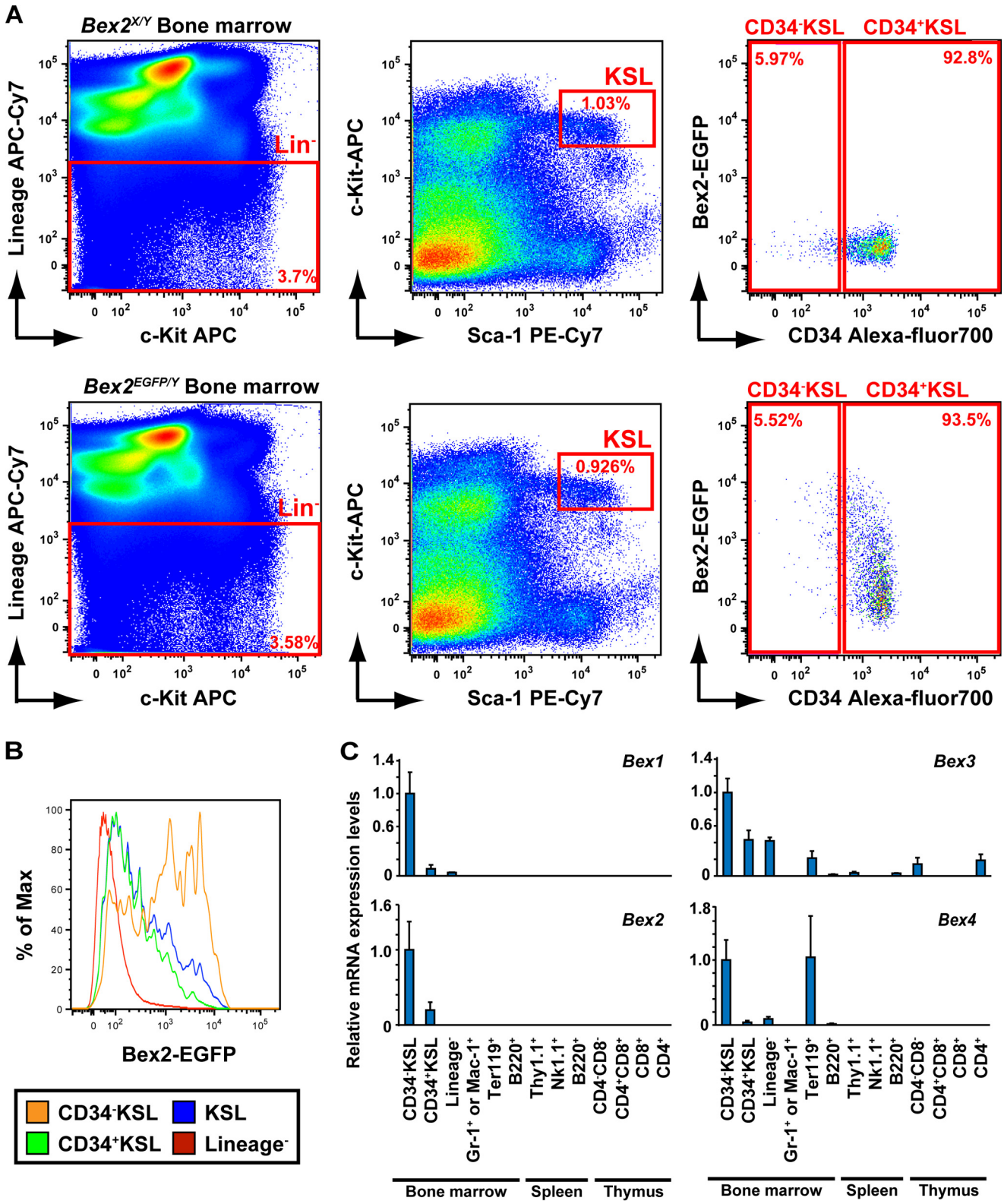

FIGURE 13. **Bex2-EGFP marks stem/progenitor cells in the hematopoietic system.** *A*, flow cytometry analysis of the bone marrow of both wild-type and *Bex2*$^{EGFP/Y}$ mice. The bone marrow cells derived from 9-week-old mice were stained and analyzed using flow cytometry. The proportions of each cell fraction did not differ significantly between wild-type and *Bex2*$^{EGFP/Y}$ mice. *Lin*$^-$, lineage negative cells; *KSL*, Lin$^-$Kit$^+$Sca1$^+$ cells; *CD34*$^-$*KSL*, Lin$^-$Kit$^+$Sca1$^+$CD34$^+$ cells; *CD34*$^-$*KSL*, Lin$^-$Kit$^+$Sca1$^+$CD34$^-$ cells. *B*, flow cytometric analysis of the bone marrow cell suspension isolated from the femurs of *Bex2*$^{EGFP/Y}$ mice. The frequency of EGFP-positive cells in the CD34$^-$KSL (*orange*), CD34$^+$KSL (*green*), KSL (*blue*), and Lineage$^-$ (*red*) fractions are shown. EGFP^{high} cells were enriched in the CD34$^-$KSL fraction. (*Lin*$^-$, lineage-negative; *KSL*, Lin$^-$Kit$^+$Sca1$^+$ cells; *CD34*$^+$*KSL*, Lin$^-$Kit$^+$Sca1$^+$CD34$^+$ cells; *CD34*$^-$*KSL*, Lin$^-$Kit$^+$Sca1$^+$CD34$^-$ cells.) *C*, quantitative PCR analysis of Bex family gene expression in fractioned wild-type hematopoietic samples. The expression in CD34$^-$KSL cells was set at 1.0. Results are presented as the mean expression levels ± S.D. of samples from three independent experiments.

cells (both $CD34^+$KSL and $Lineage^-$ cells). In particular, *Bex1* and *Bex2* were significantly expressed in $CD34^-$KSL cells, although the expression was sharply down-regulated or undetected in committed hematopoietic cells. Collectively, these results suggest that *Bex2* can be a marker of stem/progenitor cells, not only for the hepatic lineages but also for the pyloric stomach and hematopoietic tissues.

DISCUSSION

To determine the physiological role of *Bex2* and monitor the endogenous transcriptional activity of the *Bex2* genomic locus, we utilized a homologous recombination strategy. *Bex2* mRNA expression was detected in many fetal and adult tissues. However, *Bex2*-deficient mice were viable, with no apparent differences when compared with their wild-type littermates under physiological conditions. In addition, *Bex2*-deficient hepatoblasts proliferated and differentiated normally both *in vivo* and *in vitro*. Most *Bex* family genes had a similar expression pattern in both fetal and adult tissues. Of particular note, *Bex1* and *Bex2* exhibited ~90% sequence similarity and shared an extremely similar expression pattern *in vivo* (6). These findings suggest that the lack of phenotypes in *Bex2*-deficient mice may be due to the redundancy of *Bex* family genes. Therefore, generation and analyses of *Bex1* and *Bex2* double knock-out mice are of interest for future studies. In addition, because *Bex1*-deficient mice display specific phenotypes that cannot be compensated for by *Bex2* in regeneration models after injury, there may be *Bex2*-specific functions in various disease and injured processes (*e.g.* carcinogenesis, inflammation, and regeneration) as well. The role of *Bex2* in these conditions remains an intriguing topic to be explored in the near future.

Using our *Bex2* knock-out mice with the *EGFP* reporter, we were able to monitor the activation of the *Bex2* locus *in vivo*. Although we cannot completely exclude the possibility that *Bex2* is involved in its own expression, our present results showed that *Bex2* locus activation in *Bex2* knock-out mice was restricted to the cells or tissues that were positive for *Bex2* transcripts in wild-type mice. For example, the brain and testis tissues had high EGFP expression in the *Bex2* reporter mice, and these tissues also showed strong expression of *Bex2* mRNA in wild-type mice. Many researchers have attempted to identify markers that are specifically expressed in a particular cell type, *e.g.* stem cells or cells of a specific differentiated lineage. Using these mice, we found that the *Bex2* locus is not only active in the nervous system but is also specifically active in very rare cell types such as endocrine cells and several tissue stem/progenitor cells.

Although the endocrine cells of the gastrointestinal and neural systems are derived from different origins (42, 43), they express common marker genes involved in the biosynthesis of neurotransmitters and have similar ultrastructural properties (44). Moreover, it has recently been shown that the differentiation of gut endocrine cells requires the basic helix-loop-helix transcription factors MATH1, Neurogenin 3, and NeuroD as well as several Sry-box-related transcription factors (45, 46), as in the differentiation of nervous cells. Therefore, *Bex2* expression in endocrine cells might be regulated by these transcription factors, which are commonly involved in nervous cell differentiation (47). We also demonstrated that *Bex2* expression is highly correlated with the development of hepatic progenitor cells. Using several hepatic progenitor cell surface markers, such as Dlk1, CD133, CD13, and Liv2, we found that almost all of the $CD133^+Dlk1^+$ cells in E13.5 fetal livers expressed EGFP in the reporter mice. Conversely, cells expressing Bex2-EGFP at the highest levels were all positive for the hepatoblast markers and were able to form hepatic colonies in culture at very high efficiency, thus confirming the utility of this EGFP reporter as a novel hepatic progenitor marker in the fetal liver. In addition, *Bex2* also marked stem/progenitor cells of the adult pyloric epithelium and the hematopoietic system in these mice. Comparison of gene expression patterns between Bex2-EGFP-positive cells and Bex2-EGFP-negative cells in various tissues in this *Bex2-EGFP* reporter mouse may identify transcription factors and signaling molecules that are specific to these cell types and thus may lead to further understanding of the regulatory mechanisms of endocrine cell differentiation as well as the self-renewal and differentiation processes of stem/progenitor cells in future studies.

Our comparative gene expression analysis between hepatoblasts and adult hepatocytes revealed a close association of many stem/progenitor cell-specific genes and the X chromosome, similarly to the hematopoietic system (1). In addition, we found that a number of imprinted genes were specifically expressed in the stem/progenitor cells of the liver. The tight regulation of the imprinted gene network in stem cells has been documented previously in the lung (48), brain (49), and hematopoietic (50) systems. In addition, using a transgenic reporter mouse line, paternally expressed gene 3 (*Peg3*/*Pw1*), an imprinted gene located on chromosome 7, was recently shown to mark stem/progenitor cells in various tissues (38). Considering the close association between various tissue stem/progenitor cells and these X-linked and imprinted genes, the selective activation of X-linked and imprinted genes appears to be a common feature of stem/progenitor cells of various tissues. Exploring the mechanisms of how these genes, including *Bex2*, are transcribed may reveal the nature of tissue stem cells.

Collectively, by generating *Bex2-EGFP* knock-in mice, we have provided one example of using genes on the X chromosome to study neuronal/endocrine cells as well as stem/progenitor cells. This could be the basis for generating additional animal models with genetic modifications on the X chromosome for use in research in neuronal and stem cell biology.

Acknowledgments—We thank T. Nishimura, T. Shimizu, H. Masaki, and S. Kakinuma for discussions. We thank T. Mizutani and T. Nakamura for advice on enteroendocrine cells and for comments on the manuscript. We thank A. Miyajima for the kind gift of anti-CK19 antibody. We thank M. Okabe for providing EGR-101 ES cells. We thank Y. Yamazaki and A. Umino for great technical assistance on experiments. We also thank M. Kasai for critical reading of the manuscript.

REFERENCES

1. Forsberg, E. C., Prohaska, S. S., Katzman, S., Heffner, G. C., Stuart, J. M., and Weissman, I. L. (2005) Differential expression of novel potential regulators in hematopoietic stem cells. *PLoS Genet.* **1,** e28

2. Yang, F., Gell, K., van der Heijden, G. W., Eckardt, S., Leu, N. A., Page, D. C., Benavente, R., Her, C., Höög, C., McLaughlin, K. J., and Wang, P. J. (2008) Meiotic failure in male mice lacking an X-linked factor. *Gene Dev* **22,** 682–691
3. Ropers, H. H., and Hamel, B. C. (2005) X-linked mental retardation. *Nat. Rev. Genet.* **6,** 46–57
4. Jeon, C., and Agarwal, K. (1996) Fidelity of RNA polymerase II transcription controlled by elongation factor TFIIS. *Proc. Natl. Acad. Sci. U.S.A.* **93,** 13677–13682
5. Thomas, M. J., Platas, A. A., and Hawley, D. K. (1998) Transcriptional fidelity and proofreading by RNA polymerase II. *Cell* **93,** 627–637
6. Alvarez, E., Zhou, W., Witta, S. E., and Freed, C. R. (2005) Characterization of the Bex gene family in humans, mice, and rats. *Gene* **357,** 18–28
7. Brown, A. L., and Kay, G. F. (1999) Bex1, a gene with increased expression in parthenogenetic embryos, is a member of a novel gene family on the mouse X chromosome. *Hum. Mol. Genet.* **8,** 611–619
8. Behrens, M., Margolis, J. W., and Margolis, F. L. (2003) Identification of members of the Bex gene family as olfactory marker protein (OMP) binding partners. *J. Neurochem.* **86,** 1289–1296
9. Koo, J. H., Gill, S., Pannell, L. K., Menco, B. P., Margolis, J. W., and Margolis, F. L. (2004) The interaction of Bex and OMP reveals a dimer of OMP with a short half-life. *J. Neurochem.* **90,** 102–116
10. Koo, J. H., Saraswati, M., and Margolis, F. L. (2005) Immunolocalization of Bex protein in the mouse brain and olfactory system. *J. Comp. Neurol.* **487,** 1–14
11. Hofsli, E., Wheeler, T. E., Langaas, M., Laegreid, A., and Thommesen, L. (2008) Identification of novel neuroendocrine-specific tumour genes. *Br. J. Cancer* **99,** 1330–1339
12. Naderi, A., Teschendorff, A. E., Beigel, J., Cariati, M., Ellis, I. O., Brenton, J. D., and Caldas, C. (2007) BEX2 is overexpressed in a subset of primary breast cancers and mediates nerve growth factor/nuclear factor-κB inhibition of apoptosis in breast cancer cell lines. *Cancer Res.* **67,** 6725–6736
13. Zhou, X., Meng, Q., Xu, X., Zhi, T., Shi, Q., Wang, Y., and Yu, R. (2012) Bex2 regulates cell proliferation and apoptosis in malignant glioma cells via the c-Jun NH_2-terminal kinase pathway. *Biochem. Biophys. Res. Commun.* **427,** 574–580
14. Fischer, C., Drexler, H. G., Reinhardt, J., Zaborski, M., and Quentmeier, H. (2007) Epigenetic regulation of brain expressed X-linked-2, a marker for acute myeloid leukemia with mixed lineage leukemia rearrangements. *Leukemia* **21,** 374–377
15. Vilar, M., Murillo-Carretero, M., Mira, H., Magnusson, K., Besset, V., and Ibáñez, C. F. (2006) Bex1, a novel interactor of the p75 neurotrophin receptor, links neurotrophin signaling to the cell cycle. *EMBO J.* **25,** 1219–1230
16. Mukai, J., Hachiya, T., Shoji-Hoshino, S., Kimura, M. T., Nadano, D., Suvanto, P., Hanaoka, T., Li, Y., Irie, S., Greene, L. A., and Sato, T. A. (2000) NADE, a p75NTR-associated cell death executor, is involved in signal transduction mediated by the common neurotrophin receptor p75NTR. *J. Biol. Chem.* **275,** 17566–17570
17. Mukai, J., Shoji, S., Kimura, M. T., Okubo, S., Sano, H., Suvanto, P., Li, Y., Irie, S., and Sato, T. A. (2002) Structure-function analysis of NADE–identification of regions that mediate nerve growth factor-induced apoptosis. *J. Biol. Chem.* **277,** 13973–13982
18. Koo, J. H., Smiley, M. A., Lovering, R. M., and Margolis, F. L. (2007) Bex1 knock out mice show altered skeletal muscle regeneration. *Biochem. Biophys. Res. Commun.* **363,** 405–410
19. Khazaei, M. R., Halfter, H., Karimzadeh, F., Koo, J. H., Margolis, F. L., and Young, P. (2010) Bex1 is involved in the regeneration of axons after injury. *J. Neurochem.* **115,** 910–920
20. Lee, C. S., Friedman, J. R., Fulmer, J. T., and Kaestner, K. H. (2005) The initiation of liver development is dependent on Foxa transcription factors. *Nature* **435,** 944–947
21. Calmont, A., Wandzioch, E., Tremblay, K. D., Minowada, G., Kaestner, K. H., Martin, G. R., and Zaret, K. S. (2006) An FGF response pathway that mediates hepatic gene induction in embryonic endoderm cells. *Dev. Cell* **11,** 339–348
22. Hiemisch, H., Schütz, G., and Kaestner, K. H. (1997) Transcriptional regulation in endoderm development: characterization of an enhancer controlling Hnf3g expression by transgenesis and targeted mutagenesis. *EMBO J.* **16,** 3995–4006
23. Yamaguchi, T., Hamanaka, S., Kamiya, A., Okabe, M., Kawarai, M., Wakiyama, Y., Umino, A., Hayama, T., Sato, H., Lee, Y. S., Kato-Itoh, M., Masaki, H., Kobayashi, T., Yamazaki, S., and Nakauchi, H. (2012) Development of an all-in-one inducible lentiviral vector for gene specific analysis of reprogramming. *PLoS One* **7,** e41007
24. Ito, K., Yanagida, A., Okada, K., Yamazaki, Y., Nakauchi, H., and Kamiya, A. (2014) Mesenchymal progenitor cells in mouse foetal liver regulate differentiation and proliferation of hepatoblasts. *Liver Int.* **34,** 1378–1390
25. Seglen, P. O. (1979) Hepatocyte suspensions and cultures as tools in experimental carcinogenesis. *J. Toxicol. Environ. Health* **5,** 551–560
26. Ruiz i Altaba, A., Prezioso, V. R., Darnell, J. E., and Jessell, T. M. (1993) Sequential expression of HNF-3β and HNF-3α by embryonic organizing centers: the dorsal lip/node, notochord and floor plate. *Mech. Dev.* **44,** 91–108
27. Monaghan, A. P., Kaestner, K. H., Grau, E., and Schütz, G. (1993) Postimplantation expression patterns indicate a role for the mouse forkhead/Hnf-3α,β,γ genes in determination of the definitive endoderm, chordamesoderm, and neuroectoderm. *Development* **119,** 567–578
28. Ang, S. L., Wierda, A., Wong, D., Stevens, K. A., Cascio, S., Rossant, J., and Zaret, K. S. (1993) The formation and maintenance of the definitive endoderm lineage in the mouse-involvement of Hnf3/Forkhead proteins. *Development* **119,** 1301–1315
29. Lee, C. S., Sund, N. J., Behr, R., Herrera, P. L., and Kaestner, K. H. (2005) Foxa2 is required for the differentiation of pancreatic α-cells. *Dev. Biol.* **278,** 484–495
30. Okada, K., Kamiya, A., Ito, K., Yanagida, A., Ito, H., Kondou, H., Nishina, H., and Nakauchi, H. (2012) Prospective isolation and characterization of bipotent progenitor cells in early mouse liver development. *Stem Cells Dev.* **21,** 1124–1133
31. Kakinuma, S., Ohta, H., Kamiya, A., Yamazaki, Y., Oikawa, T., Okada, K., and Nakauchi, H. (2009) Analyses of cell surface molecules on hepatic stem/progenitor cells in mouse fetal liver. *J. Hepatol.* **51,** 127–138
32. Tanaka, M., Okabe, M., Suzuki, K., Kamiya, Y., Tsukahara, Y., Saito, S., and Miyajima, A. (2009) Mouse hepatoblasts at distinct developmental stages are characterized by expression of EpCAM and DLK1: drastic change of EpCAM expression during liver development. *Mech. Dev.* **126,** 665–676
33. Yamaoka, T., and Itakura, M. (1999) Development of pancreatic islets (Review). *Int. J. Mol. Med.* **3,** 247–261
34. Höcker, M., and Wiedenmann, B. (1998) Molecular mechanisms of enteroendocrine differentiation. *Ann. N.Y. Acad. Sci.* **859,** 160–174
35. Sharpe, R. M. (2006) Pathways of endocrine disruption during male sexual differentiation and masculinisation. *Best Pract. Res. Clin. Endocrinol. Metab.* **20,** 91–110
36. Sharpe, R. M., and Skakkebaek, N. E. (2003) Male reproductive disorders and the role of endocrine disruption: Advances in understanding and identification of areas for future research. *Pure Appl. Chem.* **75,** 2023–2038
37. Barker, N., Tan, S., and Clevers, H. (2013) Lgr proteins in epithelial stem cell biology. *Development* **140,** 2484–2494
38. Besson, V., Smeriglio, P., Wegener, A., Relaix, F., Nait Oumesmar, B., Sassoon, D. A., and Marazzi, G. (2011) PW1 gene/paternally expressed gene 3 (PW1/Peg3) identifies multiple adult stem and progenitor cell populations. *Proc. Natl. Acad. Sci. U.S.A.* **108,** 11470–11475
39. Barker, N., Huch, M., Kujala, P., van de Wetering, M., Snippert, H. J., van Es, J. H., Sato, T., Stange, D. E., Begthel, H., van den Born, M., Danenberg, E., van den Brink, S., Korving, J., Abo, A., Peters, P. J., Wright, N., Poulsom, R., and Clevers, H. (2010) Lgr5(+ve) stem cells drive self-renewal in the stomach and build long-lived gastric units *in vitro*. *Cell Stem Cell* **6,** 25–36
40. Osawa, M., Nakamura, K., Nishi, N., Takahasi, N., Tokuomoto, Y., Inoue, H., and Nakauchi, H. (1996) *In vivo* self-renewal of c-Kit(+) Sca-1(+) Lin(low/−) hemopoietic stem cells. *J. Immunol.* **156,** 3207–3214
41. Osawa, M., Hanada, K., Hamada, H., and Nakauchi, H. (1996) Long-term lymphohematopoietic reconstitution by a single CD34-low/negative hematopoietic stem cell. *Science* **273,** 242–245
42. Andrew, A., Kramer, B., and Rawdon, B. B. (1983) Gut and pancreatic amine precursor uptake and decarboxylation cells are not neural crest derivatives. *Gastroenterology* **84,** 429–431

43. Andrew, A., Kramer, B., and Rawdon, B. B. (1998) The origin of gut and pancreatic neuroendocrine (APUD) cells–the last word? *J. Pathol.* **186,** 117–118
44. Pearse, A. G. (1969) Cytochemistry and ultrastructure of polypeptide hormone-producing cells of apud series and embryologic physiologic and pathologic implications of concept. *J. Histochem. Cytochem.* **17,** 303–313
45. Li, H. J., Ray, S. K., Singh, N. K., Johnston, B., and Leiter, A. B. (2011) Basic helix-loop-helix transcription factors and enteroendocrine cell differentiation. *Diabetes Obes. Metab.* **13,** 5–12
46. McDonald, E., Krishnamurthy, M., Goodyer, C. G., and Wang, R. (2009) The emerging role of SOX transcription factors in pancreatic endocrine cell development and function. *Stem Cells Dev.* **18,** 1379–1388
47. Hagens, O., Dubos, A., Abidi, F., Barbi, G., Van Zutven, L., Hoeltzenbein, M., Tommerup, N., Moraine, C., Fryns, J. P., Chelly, J., van Bokhoven, H., Gécz, J., Dollfus, H., Ropers, H. H., Schwartz, C. E., de Cassia Stocco Dos Santos, R., Kalscheuer, V., and Hanauer, A. (2006) Disruptions of the novel KIAA1202 gene are associated with X-linked mental retardation. *Hum. Genet.* **118,** 578–590
48. Zacharek, S. J., Fillmore, C. M., Lau, A. N., Gludish, D. W., Chou, A., Ho, J. W., Zamponi, R., Gazit, R., Bock, C., Jäger, N., Smith, Z. D., Kim, T. M., Saunders, A. H., Wong, J., Lee, J. H., Roach, R. R., Rossi, D. J., Meissner, A., Gimelbrant, A. A., Park, P. J., and Kim, C. F. (2011) Lung stem cell self-renewal relies on BMI1-dependent control of expression at imprinted loci. *Cell Stem Cell* **9,** 272–281
49. Ferrón, S. R., Charalambous, M., Radford, E., McEwen, K., Wildner, H., Hind, E., Morante-Redolat, J. M., Laborda, J., Guillemot, F., Bauer, S. R., Fariñas, I., and Ferguson-Smith, A. C. (2011) Postnatal loss of Dlk1 imprinting in stem cells and niche astrocytes regulates neurogenesis. *Nature* **475,** 381–385
50. Venkatraman, A., He, X. C., Thorvaldsen, J. L., Sugimura, R., Perry, J. M., Tao, F., Zhao, M., Christenson, M. K., Sanchez, R., Yu, J. Y., Peng, L., Haug, J. S., Paulson, A., Li, H., Zhong, X. B., Clemens, T. L., Bartolomei, M. S., and Li, L. (2013) Maternal imprinting at the H19-Igf2 locus maintains adult haematopoietic stem cell quiescence. *Nature* **500,** 345–349